Received: 14 December 2022 | Revised: 6 March 2023 | Accepted: 30 March 2023

DOI: 10.1002/smm2.1215

SmartMat Open Access WILEY

REVIEW

Intelligent ion gels: Design, performance, and applications

Naiwei Gao[1,2] | **Caofeng Pan**[1,3]

[1]Beijing Key Laboratory of Micro-nano Energy and Sensor, CAS Center for Excellence in Nanoscience, Beijing Institute of Nanoenergy and Nanosystems, Chinese Academy of Sciences, Beijing, China

[2]Key Laboratory of Optoelectronic Devices and Systems of Ministry of Education, Center for Stretchable Electronics and Nano Sensors, College of Physics and Optoelectronic Engineering, Shenzhen University, Shenzhen, China

[3]School of Nanoscience and Engineering, University of Chinese Academy of Sciences, Beijing, China

Correspondence
Caofeng Pan, Beijing Key Laboratory of Micro-nano Energy and Sensor, CAS Center for Excellence in Nanoscience, Beijing Institute of Nanoenergy and Nanosystems, Chinese Academy of Sciences, Beijing 101400, China.
Email: cfpan@binn.cas.cn

Funding information
Fundamental Research Funds for the Central Universities; Natural Science Foundation of Beijing Municipality, Grant/Award Number: Z180011 and 2222088; Shenzhen Science and Technology Program, Grant/Award Number: KQTD20170810105439418; National key R&D program of China, Grant/Award Number: 2021YFB3200302 and 2021YFB3200304; National Natural Science Foundation of China, Grant/Award Numbers: 52125205, U20A20166 and 52192614; China Postdoctoral Science Foundation, Grant/Award Number: 2021M692185

Abstract

Intelligent ion gels, which possess highly tunable mechanical, electrical, and stimulus-responsive properties, have emerged as powerful candidates in the field of artificial intelligence, telemedicine, and health monitoring. To enrich the functionality of ion gels, it is critical to explore the link between the structure and function of ion gels. In this review, we provide an overview of the synthesis path and functional derivatives of ion gels. The conformational relationships of ion gels have been discussed, such as the effect of structure on electrical conductivity as well as sensing properties. From the perspective of stimulus response, the role of ion gels in areas such as bionic haptics, neural devices, artificial muscles, and intelligent displays has also been explored. It is possible that smart ion gels will open up a new horizon in the upcoming smart era, especially after the current challenges are resolved.

KEYWORDS

chemical structure, intelligent electronics, ion gels, stimulus-responsive

1 | INTRODUCTION

Ion conduction, the most important mode of transmission of biological signals, is widely involved in the regulation of physiological activities, including tactile perception, muscle movement, nerve conduction, and even hormone secretion.[1–6] As is known, common electronic devices usually transmit signals based on electrons and holes. However, researchers found that ion channel proteins, which play a key role in ion conduction, can also respond to specific external stimuli precisely.[7] When being stimulated by special signals, corresponding channel proteins can selectively pass through the targeting ion species, thus realizing various biological functions. Mimicking of the structure and functions of the human body is crucial for the promotion of existing smart electronics. For the first time, the bionic perception of the skin's sense of touch has been studied

---

based on many different types of flexible electronic materials with excellent performance.[8–13] Researchers[14–16] developed flexible circuits based on inorganic silicon topologies. Hammock et al.[17] and Wang et al.[18] proposed the concept of an "electronic skin" in the design of flexible organic semiconductor devices. Ionic materials, based on different conductive mechanism, also served as the ideal materials for bionic skin. In 2014, Suo and colleagues[19] proposed the concept of an "ionic skin" based on ionic conductive materials. Compared with electronic devices, the ionic skin mainly has a skin-like ionic conduction mechanism in an electric field. The transmission mechanism of ionic devices is more like that of living organisms, which is theoretically more likely to improve sensor performance, as well as the interface transmission and signal integration between ionic devices and living organisms. It should be noted that ionic devices are still in the early stages of development. As proposed in "Iontronics: Ionic Carriers in Organic Electronic Materials and Devices,"[20–26] the existing ionic devices are still based on the concept of "ionic electronic devices." All ionic devices need to be integrated with electronic devices. In practice, two different types of carrier transport (electrons and ions) are involved at the interface between ionic and electronic conductors. Therefore, current ionic devices are not completely free from the requirement of electron carrier transport. In-depth studies of ion conduction mechanisms and exploration of the relationship between ionic structures and functions are still of great scientific importance.

Structurally, both gels contain a polymer backbone and a liquid component within the gel. In terms of ion conduction mechanisms, both hydrogels and ion gels contain free-moving ionic carriers within them, which can be used to create "ionic skins." The main difference is that the liquid inside the hydrogel is mainly water, while the liquid inside the ion gel includes ionic liquids (ILs). Due to the high saturated vapor pressure of water, hydrogels usually undergo water loss when exposed to air.[27] However, for ion gels, the ILs within the gels have the superior advantage of negligible saturated vapor pressure. The problem of water loss can be naturally avoided because the preparation of ion gels does not require the use of water. As stated, ion gels can be divided into two parts: the gel skeleton and ionic components. The gel skeleton mainly includes various polymer skeletons and inorganic hybrid materials, and the ionic components mainly consist of ILs with different functions. Previous studies have confirmed that ion gels have major advantages of stimuli responsiveness, high transparency, stretchability, biocompatibility, modulus tunability, and structural designability.[28,29] Additionally, the introduction of ILs further endows ion gels with other advantages of negligible saturation vapor pressure, high thermal stability, a wide electrochemical window, and high ionic conductivity.[30] In recent years, ion gels have become the mainstream materials in the fields of multifunction electronics and smart electronics. Many reviews have summarized the development of ion gels in the fields of gel synthesis, ion transport mechanisms, and transport at the ion/electron interface, which have greatly enhanced the understanding of ion gels in related fields.[31-34] However, the relationship between the smart response of ion gels and their structure has still not been outlined systematically. It is very important to explore the relationship between the components of ion gels and their stimulus response for the design of multifunctional ion gels.

In this review, we will focus on the structural design of ion gels to explore the structure–property relationship of stimulus-responsive ion gels. The synthesis method of ion gels will be discussed from the viewpoint of the form of ionic components in ion gels. The focus is on ionic conductivity here owing to its crucial function in the design of ion gel-based smart devices. Next, the stimulus responsiveness of ion gels is explored based on the relationship between the chemical structure of ion gels and the external stimulus, which is divided into physical signals and chemical signals according to their signal forms. The following section will describe the intelligent applications of stimulus-responsive ion gels in biomimicking haptics, artificial muscles, smart display devices, and so on. Finally, we will summarize this review and offer some perspectives on the potential future research avenues, advancement, and applications of ion gels. In addition, the existing challenges of ion gels will also be discussed.

2 | SYNTHESIS OF ION GELS

According to the structures of ion gels with different functions, the synthesis routes of ion gels can be divided into four types, including physical blending, radical polymerization, supramolecular polymerization, and nanocomposites. Since most ILs have a melting point below room temperature (298.15 K) and are inherently fluid, the preparation of ion gels using ILs can avoid the introduction of aqueous solvents. At the same time, ILs inherently have high ionic conductivity (1.00–10.0 mS/cm), which allows ion gels to be prepared according to the actual application requirements. For example, when ion gels are used as electrodes, high conductivity is usually required, which can reduce the interfacial resistance and induce improvement in the accuracy and precision of signal acquisition. However, when ion gels are used as smart sensors, the sensitive responsiveness of the external stimulus becomes more important, and this process usually does not require that ion gels have very high ionic conductivities (unless stated specifically, the conductivity mentioned in this review is the room-temperature conductivity).

2.1 | Polymer blended with ILs

The simplest process for preparing ion gels is to dissolve a polymer with corresponding solvents and then directly blend it with ILs (Figure 1A).[35] The classical polymer that is utilized for ion skeletons mainly has a relatively low molecular mass, for example, poly(vinylidene fluoride) (PVDF),[37] poly(vinyl alcohol) (PVA),[38] poly(methyl methacrylate) (PMMA),[39] poly(ethylene glycol) (PEG),[40] DNA,[41] and so on. Since ILs exist in the form of liquid ion gels, ion gels prepared via physical blending can have high ionic conductivity, usually reaching 1.00 mS/cm. Some ion gels can even reach 9.00 mS/cm. The ionic conductivity of ion gels depends mainly on the concentration of free anions and cations, which can move under certain electric fields. This free migration of ions is mainly linked to the entanglement of polymer molecular chains and the content of ILs loaded in ion gels. For instance, Sun and colleagues[42] synthesized an ion gel by mixing a tetrahydrofuran (THF) solution dissolved with polyurethane (PU) and an ethanol solution dissolved with 1,2-dimethyl-3-ethoxyethyl-imidazolium bis(trifluoromethanesulfonyl) imide ([DEIm][TFSI]). The mass ratio of ILs to the PU network is 2:1. Here, the ionic conductivity of the ion gels could reach 1.20 mS/cm, and the performance could remain stable for 200 days when placed in a natural environment. This can be attributed to the good compatibility between the structure of the amide bond in PU and [DEIm][TFSI]. In addition, McFarlane and colleagues[43] found that ion gels composed of poly(tetrafluoroethylene) (PTFE) and 1-ethyl-3-methylimidazolium bis(trifluoromethylsulfonyl)imide ([EMIm][TFSI]) can also reach a relatively high ionic conductivity of 1.01 mS/cm. The good compatibility between PTFE and ILs is considered to be responsible for this high ionic conductivity. It can be confirmed that improving the interaction between the polymer chain and ILs can induce improved ionic conductivity of ion gels. Another method that can be used to enhance the conductivity of ion gels is the use of ionic components with high ionic conductivity. Pandey et al.[44] blended 1-ethyl-3-methylimidazolium thiocyanate ([EMIm][SCN]) with polyacrylonitrile (PAN) in a solvent to obtain an ion gel with super-high ionic conductivity of 10.0 mS/cm. In addition to the good compatibility between two components, the high ionic conductivity of [EMIm][SCN] (14.0 mS/cm) also plays a crucial role in the synthesis of conductive ion gels. In addition, deep eutectic solvents (DESs), a special type of ILs, can also be used as an ionic component of ion gels. DESs also have many advantages of ILs, such as low saturation vapor pressure, high ionic conductivity, and so on. Panzer and colleagues[45] prepared ion gels with an ionic conductivity of 2.5 mS/cm and elongation over 300% by coblending choline chloride (ChCl), ethylene glycol (EG), and gelatin.

Although polymer dissolution is a simple process with low cost of preparation, it is only suitable for linear polymers. For bulk polymers, the polymer chains are covalently cross-linked, making it difficult for the solvents to penetrate (Figure 1B).[36] Blending ILs with polymer monomers, followed by polymerization is an effective strategy to prepare bulk polymer-based ion gels. However, although increasing the contents of ILs can increase the ionic conductivity of ion gels, excessive use of ILs may also reduce the mechanical properties of ion gels. In some severe cases, it can even completely inhibit the polymerization of the polymer matrix. Considering the commonly used poly(dimethylsiloxane) (PDMS) as an example, the Young's modulus of a pure PDMS film is 1.00 MPa. On adding 20.0 wt% by mass of [EMIm][TFSI] to a PDMS prepolymer, the Young's modulus of the PDMS-based ion gel is reduced to 0.01 MPa.[46]

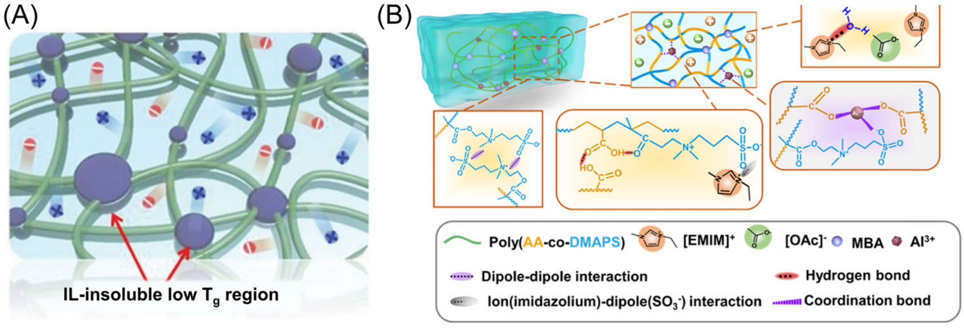

FIGURE 1 (A) Ion gels based on linear polymers. Reproduced with permission: Copyright 2019, Wiley-VCH.[35] (B) Ion gels based on cross-linking polymers. Reproduced with permission: Copyright 2022, American Chemical Society.[36]

Horowitz and Panzer[47] used formic acid (FA) as a cosolvent to inhibit the phase separation between a PDMS prepolymer and three different ILs, including [EMIm][TFSI], 1-butyl-3-methylpyrrolidinium bis(trifluoromethylsulfonyl) imide ([BMP][TFSI]), and 1-ethyl-3-methylimidazolium tetracyanoborate bis(trifluoromethylsulfonyl)imide ([EMIm][TCB]). Using this method, ion gels with high contents of ILs were prepared. The ionic conductivity of the ion gels obtained after solvent evaporation could reach 3.00 mS/cm and their Young's modulus could reach 0.06 MPa. Wang and colleagues[48] prepared porous PDMS sponges using square sugar as a template to adsorb ILs into the interior of PDMS by the capillary effect of pores. The design of porous ion gels is expected to further enhance the loading of ILs in ion gels, thus achieving higher ionic conductivity while retaining the mechanical properties of ion gels.

2.2 | Polymerizing double-bond-containing ILs

Due to the strong molecular designability of ILs, it is easy to replace the substituents of ILs with those containing double bonds by a "one-step" nucleophilic reaction. In fact, the commercial 1-vinyl-3-methylimidazolium chloride salt ([VMIm][Cl]) is synthesized in this way. The introduction of double bonds allows ILs to form PILs directly by means of free radical polymerization, cationic polymerization, or RAFT polymerization. The ion gels can effectively avoid the phase separation problem caused by physical copolymerization and promote more homogeneous and stable ion distribution of ion gels.

Limited to the ionic structure of ILs, PILs synthesized entirely from the polymerization of ILs often have poor mechanical and electrical properties. To improve the properties of PILs, their preparation often involves the copolymerization of multiple polymer monomers. Although Zhang et al.[49] reported improved modulus and mechanical strength based on one-component PILs by extending the side chain length of imidazolium cationic substituents, multicomponent PILs still remain a hot topic of research. As shown in Figure 2A, Watanabe and colleagues[50] designed two double-bond-substituted ILs 1-[(3-methacryloyloxy) propyl]-3- methylimidazolium bis(trifluoromethane sulfonyl)amide ([C3mimMA][TFSA]) and 1-methyl-3-propylimidazolium *N*-[3-(methacryloyloxy)propylsulfonyl]-*N*- (trifluoromethanesulfonyl) amide ([C3mim] [TFSA-MA]). Further

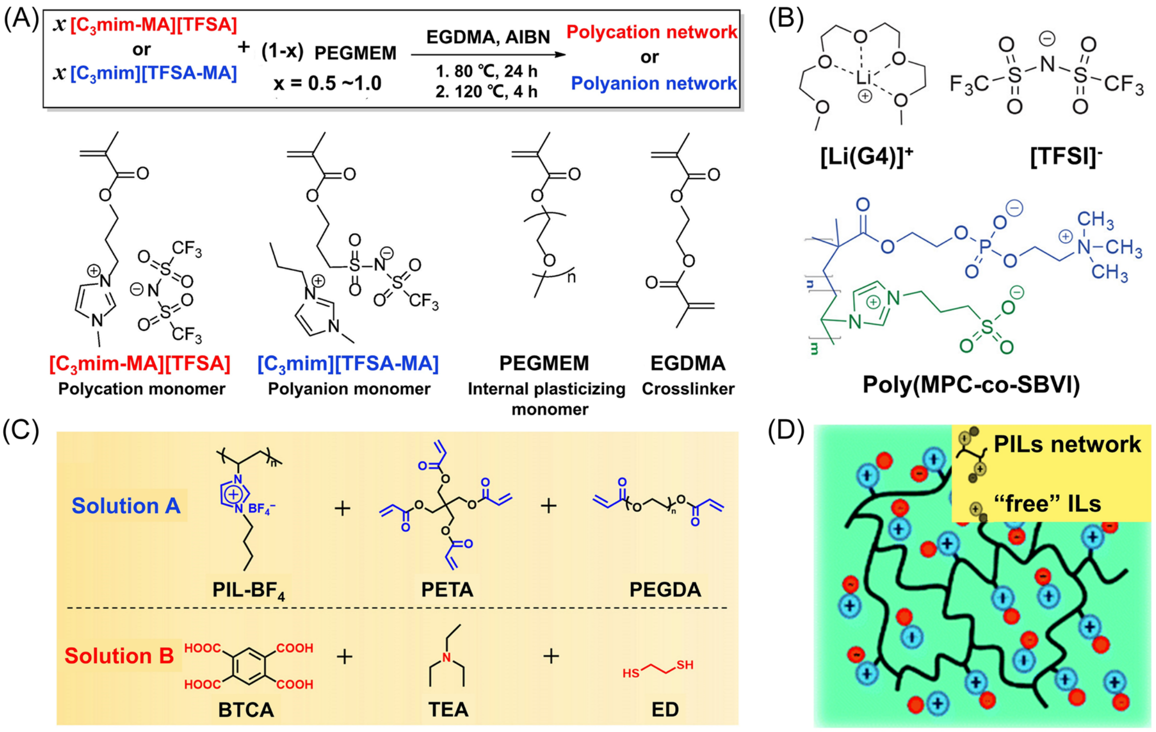

FIGURE 2 (A) Preparation of multicomponent PILs. Reproduced with permission: Copyright 2018, Elsevier Ltd.[50] (B) Ion gels composed of PILs and gel factors. Reproduced with permission: Copyright 2019, American Chemical Society.[51] (C) The two solutions for the synthesis of the click-ion gels. Reproduced under the terms of the Creative Commons Attribution-NonCommercial license: Copyright 2019, American Association for the Advancement of Science.[52] (D) The ion gels prepared using the emulsion-templated method. Reproduced with permission: Copyright 2018, Royal Society of Chemistry.[53]

copolymerization of these ILs and other polymers, such as poly[(ethylene glycol) methyl ether methacrylate] (PEGMEM) and ethylene glycol dimethacrylate (EGDMA), can yield ion gels with an ionic conductivity range of 10^{-3} to 10^{-4} mS/cm. Remarkably, PIL-based ion gels reduce the ionic conductivity because the free migration of ions is limited. The polymerization immobilizes the anions or cations in the ion gel backbone in the form of covalent bonds. To improve the ionic conductivity, D'Angelo and Panzer[51] dissolved two amphoteric IL monomers, 2-methacryloyloxyethyl phosphorylcholine (MPC) and sulfobetaine vinylimidazole (SBVI), in a third IL lithium-tetraglyme bis(trifluoromethylsulfonyl)-imide ([Li(G4)][TFSI]) (Figure 2B). After radical copolymerization, ion gels with a conductivity of 1.34 mS/cm could be obtained. In Figure 2C, it can be seen that Ren et al.[52] designed a click-ion gel with a superhigh conductivity of 83.0 mS/cm and excellent mechanical properties, which is different from the conventional PIL preparation process. Here, two different precursor solutions were blended to form click-ion gels. One solution is composed of the polymer of poly (ethylene glycol) diacrylate (PEGDA), the cross-linker of pentaerythritol tetra-acrylate (PETA), and anionic BTCA in methanol. The other solution consists of the PILs (PIL-BF_4), the catalyst of triethylamine (TEA), and 1,2-ethanedithiol (ED) in methanol. The method is based on the thiol-ene click reaction. As shown in Figure 2D, the emulsion-templated approach was developed by Debuigne and colleagues[53] Many other methods for the preparation of poly(ion gels) have been developed, such as initiated chemical vapor deposition (iCVD) and 3D printing.

2.3 | Supramolecular ion gels

Due to the advantages of the ionic structure as well as fluidic properties of ILs, supramolecular interactions have become another important means of preparing ion gels. Owing to the dynamic reversibility of hydrogen bonds, coordination bonds, van der Waals interactions, π–π interactions, and hydrophobic interactions, supramolecular ion gels are expected to play an important role in transient electronic devices, recyclable sensors, reconfigurable circuits, and multimode sensing.

A previous study proved that $[TFSI]^-$ anions can form host–guest supramolecular complexes with cyclodextrins (CDs). In Figure 3A, Yan and colleagues[54] assembled PILs containing $[TFSI]^-$ in a water solution of CDs to obtain supramolecular ion gels with a shape memory function. As shown in Figure 3B, Yamaguchi and colleagues[55] further covalently grafted CDs onto the side chains of a polymer and assembled them with [EMIm][TFSI] in host–guest complexes to obtain ion gels. Thanks to the supramolecular interactions in the ion gels, the ionic conductivity of the ion gels can be as high as 8.00 mS/cm, which is almost the same as the ionic conductivity of [EMIm][TFSI] (9.00 mS/cm). The possibility of constructing supramolecular ion gels was also analyzed using the grand-reaction method. These supramolecular gels are mainly based on electrostatic selfassembly, and their assembly process is susceptible to the pH environment of the solution (Figure 3C).[56] In Figure 3D, it can be seen that D'Anna and colleagues[57] designed an IL composed of high-valence anions and cations, diimidazolium ethylenediaminetetraacetate ($[p\text{-}C_{12}Im]_2[Edta]$), by the derivation of di-3,3′-di-n-dodecyl-1,1′-(1,4-phenylenedimethylene). A series of gel factor didodecylimidazolium-based ($[C_{12}C_{12}Im]^+$) salts with electrostatic interactions with ILs, including 1,4 benzenedicarboxylate ([1,4-BDC]), 2,6-naphthalenedicarboxylate ([2,6-NDC]), trimesate ([Trim]), and citrate ([Cit]), were also prepared to form ion gels with high performance (Figure 3E).[58] Zhao et al.[59] proposed a “hydrogen-bond topological network” design approach (Figure 3F). When the water content was reduced, the intermolecular hydrogen bonds of cellulose were broken by the surrounding anions and imidazole cations. In this state, the molecular topological network was weak, and the ionic conductivity was about 7.6 mS/cm. When the water content of the ion gel was increased, a strong hydrogen-bond topological network was formed between water molecules and cellulose. In the new state, the ionic conductivity could be increased to 38.5 mS/cm. Wang and colleagues[60] constructed self-healing and recyclable supramolecular ion gels based on the tetrameric hydrogen-bonding group 2-ureido-4-[1H] pyrimidinone (UPy). π–π interactions, as important supramolecular interactions, were also successfully used to prepare supramolecular ion gels. For example, Wang and colleagues[61] synthesized imidazolium ILs containing azo-phenyl groups, which can form supramolecular ion gels with reconfigurable properties by crystal-confined assembly with conventional ILs.

2.4 | Inorganic ion gels

The preparation process of inorganic ion gels is very similar to that of polymer-blended ion gels. Inorganic ion gels are usually made up of inorganic gelation factors such as carbon nanotubes, graphene, titanium dioxide nanoparticles, and inorganic silicon nanoparticles. Compared with physical coblending, PILs, and supramolecular ion gels, inorganic ion gels usually have a plastic state with poor mechanical strength and are often used to prepare sol–gel transition systems. Many studies have confirmed that carbon nanotubes have good

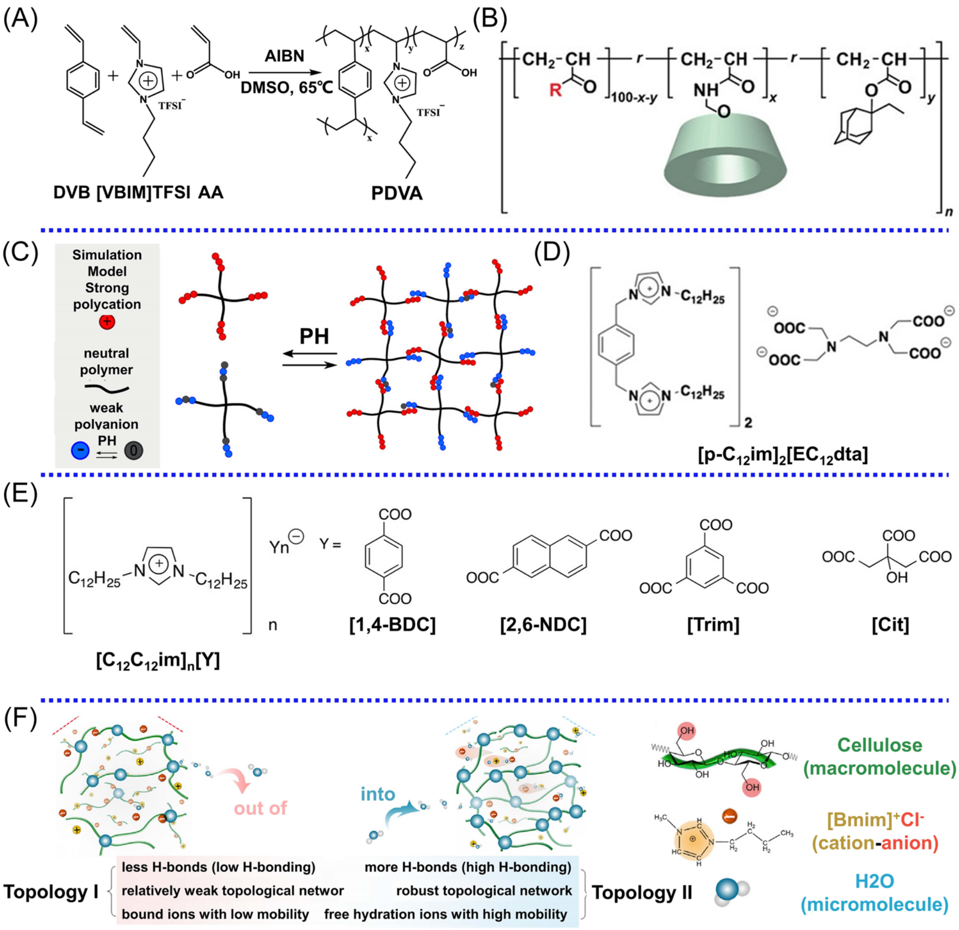

FIGURE 3 (A) Synthesis route of PILs with $[TFSI]^-$ anions. Reproduced with permission: Copyright 2014, Elsevier Ltd.[54] (B) Structure of the polymer grafted with cyclodextrins (CDs). Reproduced with permission: Copyright 2019, American Chemical Society.[55] (C) Electrostatic assembly of the poly(cationic electrolytes) and poly(anionic electrolytes). Reproduced with permission: Copyright 2021, American Chemical Society.[56] (D) Gel factors composed of high-valence cations and anions. Reproduced with permission: Copyright 2019, American Chemical Society.[57] (E) Structure of the didodecylimidazolium-based salts. Reproduced with permission: Copyright 2018, American Chemical Society.[58] (F) Illustration of the strategy of the hydrogen-bond topological network. Reproduced with permission: Copyright 2019, Elsevier Inc.[59]

dispersion in ILs. Kim and colleagues[62] prepared inorganic ion gels with a stretchability of 350% by dispersing single-walled carbon nanotubes (SWCNTs) in ILs (Figure 4A). Unfortunately, as mentioned above, the stretching process is inelastic. This ion gel cannot recover to its initial state spontaneously. In Figure 4B, it can be seen that Gruttadauria and colleagues[63] prepared silica-based ionic gels by covalently modifying the IL 1-(3-trimethoxysilylpropyl)-2,3-dimethylimidazolium tetrafluoroborate onto the surface of silica nanoparticles. Martinelli and colleagues[65] investigated the sol–gel transition behavior of silica-based ion gels. It was found that the concentration of ILs, especially the anion $[TFSI]^-$, plays a very important role in the gel–sol transition. As shown in Figure 4C, Wu and colleagues[64] introduced metal ions into ion gels and obtained a new class of inorganic ion gels based on polyoxometalate-based ILs (POM-ILs), such as $[TBDA]_5SiW_{11}VO_{40}$, $[TBTA]_5SiW_{11}VO_{40}$, and $[TBTP]_5SiW_{11}VO_{40}$. Generally, these kinds of ion gels can only be used to fabricate smart electronics unless their mechanical performance can be improved.

2.5 | Comparison of several synthesis routes

Here, we briefly summarize the advantages and disadvantages by comparing four different routes for ion gel synthesis. Since this review focuses on the sensing properties of ion gels, here, we focus on the ionic conductivity as well as the stability of ion gels. As summarized in Table 1, the ion gels obtained by both physical copolymerization and supramolecular

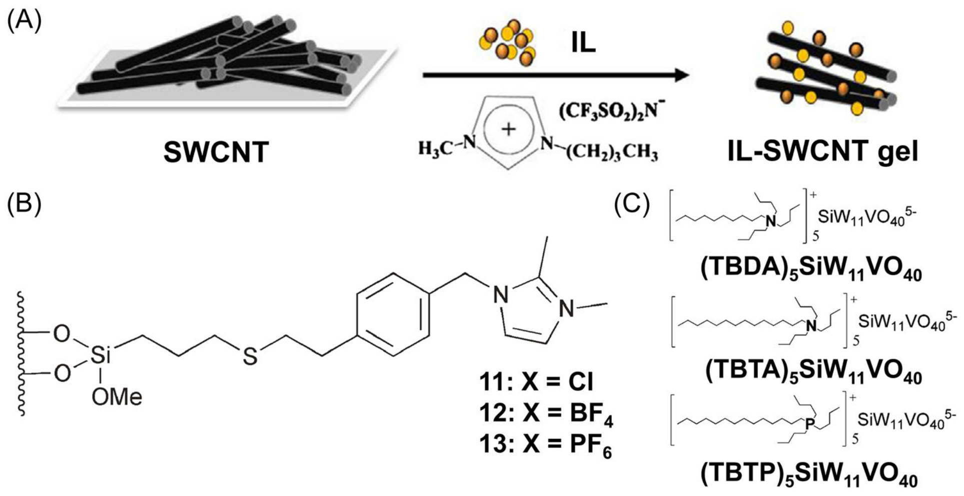

FIGURE 4 (A) Preparation process of the ion gels based on carbon nanotubes. Reproduced with permission: Copyright 2013, Elsevier Ltd.[62] (B) Structure of IL-grafted silica particles. Reproduced with permission: Copyright 2007, Royal Society of Chemistry.[63] (C) Structure of polyoxometalate-based ILs. Reproduced with permission: Copyright 2015, Royal Society of Chemistry.[64]

TABLE 1 Comparison of several synthesis routes.

Components	Synthesis routes	Phase separation	Bonding mode	Conductivity (mS/cm)	Reference
PU and [DEIm][TFSI]	p. b.	Yes	Van der Waals force	1.20	[42]
ChCl and EG and gelatin	p. b.	Yes	Electrostatic interaction	2.50	[45]
PAN and [EMIm][SCN]	p. b.	Yes	Electrostatic interaction	10.0	[44]
PDMS and [EMIm][TFSI]	p. b.	Yes	Van der Waals force	3.00	[47]
PEGMEM and [C3mimMA][TFSA]	r. p.	No	Covalent linkage	0.001	[50]
SBVI and [Li(G4)][TFSI]	r. p.	No	Covalent linkage	1.34	[51]
Click-ion gel	r. p.	No	Covalent linkage	83.0	[52]
Polymer-CD and [EMIm][TFSI]	s. p.	Yes	Host–guest interaction	8.00	[55]
Cellulose and [BMIm]Cl	s. p.	Yes	Hydrogen bond	38.5	[59]
SWCNT and IL	nm.	Yes	Van der Waals force	-	[62]
Silica and IL	nm.	Yes	Covalent linkage	-	[65]

Note: Herein, the phase separation mainly refers to the separation of the polymer skeleton and solvents. The full name of the abbreviated compounds in this table can be found in the above text. nm., nanocomposites; p. b., physical blending; r. p., radical polymerization; s. p., supramolecular polymerization.

polymerization possess high ionic conductivity. Covalent linkages are, in principle, not favorable for ion migration inside the gel, although some unique designs, for example, click gels, can also achieve high conductivity. As far as the stability of ion gels is concerned, covalently linked gels are able to suppress phase separation of the IL and the polymer backbone to the maximum extent possible, enhancing the stability of the device. The other three synthetic routes (including physical copolymerization, supramolecular polymerization, and nanoparticle composite) suffer from more severe phase separation, which is detrimental to the long-term use of the devices.

3 | STIMULUS RESPONSIVENESS

ILs are entirely made up of anions and cations that are based on weak electrostatic interactions. By changing the species of ions, the properties of ILs can also be tuned. In theory, some ILs can reach 10^{18}. This is very beneficial for the functional derivatization of ion gels. Besides, a functional polymer skeleton can also be used to improve the performance of ion gels. The interaction between the polymer skeleton and ion gels can be regarded as the third variable that can adjust the function of ion gels. Moreover, after preparing ILs in ionic gels, they can often be endowed with additional mechanical as well as electrical properties. Based on this, researchers can design a series of stimuli-responsive ion gels with different functions.

3.1 | Physical signals

The physical signals that have been widely investigated include temperature, pressure, strain, light, magnetic signals, etc. Among them, the most typical physical signals are temperature and pressure signals, which are external stimuli used in the field of haptic bionics.

The temperature response mechanisms of ion gels are mainly as follows: (i) Temperature effect of ion pair decoupling–coupling. For the ionic components in ion gels, cations and anions are mainly in the form of neutral ion pairs at room temperature. Only a few dissociative ions can migrate freely. As shown in Figure 5A, when the temperature increases, the electrostatic interactions between anions and cations are disrupted.[66] The neutral ion pair becomes the freely migrating anions and cations. This causes an increase in the ion concentration and results in an increase in the ionic conductivity of the ion gel. In fact, most ionic temperature sensors follow this mechanism. (ii) Sol–gel transition mechanism. As shown in Figure 5B, ion gels based on a thermally reversible ABC-triblock copolymer (poly (benzyl methacrylate) (PBnMA) and poly(methyl methacrylate) (PMMA) and poly(2-phenylethyl methacrylate) (PPhEtMA)) and ILs are able to undergo sol–gel transition at different temperatures.[67] The sol–gel transition consists of two processes. In the first stage, the gel's temperature is increased to 70°C, because of which the gelation process is mainly derived from the self-assembly of micelles of PPhEtMA. The gelation process is further intensified by further increasing the temperature to 105°C since the spherical micelles were transformed into dendritic micelles at higher temperature.[72] (iii) Critical temperature effect of ion gels. For example, the ion gels obtained from poly(N-isopropylacrylamide) (PNIPAAm) and ILs show lowest critical solution temperature (LCST) behavior in an aqueous environment with a phase transition temperature of 32°C (Figure 5C).[68] When the temperature is higher than 32°C, phase separation between the ion gel and water occurs and a new ion pathway is formed inside the gel. At this point, the increase in the ion concentration leads to an increase in ionic conductivity, thus achieving a response to temperature. Corresponding to LCST, the upper critical solution temperature (UCST) can also be used to prepare temperature-responsive ion gels (Figure 5E).[68] (iv) Temperature-responsive dynamic covalent bonding. The temperature response of ion gels can be achieved by the construction of temperature-responsive dynamic covalent bonds in ion gels. Fan and colleagues[69] covalently attached furan molecules and maleimide molecules, which are capable of the DA reaction, to an ion gel backbone to achieve dynamic covalent crosslinking of the ion gel backbone (Figure 5D). When the temperature was 70°C, the dynamic covalent bonds were cross-linked and the mechanical properties of the ion gels could be enhanced. When the temperature was increased to 110°C, the dynamic covalent bonds were broken and the mechanical strength of ion gels weakened. (v) Supramolecular response mechanism. Supramolecular interactions between $[TFSI]^-$ and CDs were discussed in the section on the preparation of supramolecular gels. In Figure 5F, it is shown that the supramolecular interactions between $[TFSI]^-$ and CDs can be regulated by temperature.[70] When the temperature increases, supramolecular interactions are disrupted and the modulus of ion gels decreases. When the temperature decreases, the supramolecular interaction can be re-established. (vi) The Soret effect. The phenomenon of thermal diffusion of ionic components from the high-temperature end to the low-temperature end under a temperature gradient is called the Soret effect (Figure 5G).[71] It is known that the migration rates of different anions and cations of ionic components are different due to the differences in volume and functional groups, and so on. This leads to differences in the concentrations of anions and cations at the cold and hot ends. As a result, a certain voltage can emerge at the cold and hot ends. The difference in voltage can then be used to determine the range of the ambient temperature.

Different from the temperature response, the pressure response of ion gels is not only influenced by the structure and property of ion gels. Here, the device design is more important for the realization of sensitive pressure response. There are four main pressure response mechanisms of ion gels, including piezoresistive, piezoelectric, capacitive, and triboelectric. Since these four pressure response mechanisms have been summarized in numerous reviews, we will not introduce them in detail here, but the ion gel-based pressure sensors that have emerged in recent years will be introduced in the next chapter.

In addition to temperature and pressure signals, ion gels that respond to light have excellent potential for use in applications in biomolecular recognition, chemical sensing, and fluorescence imaging. By introducing light-responsive gel factors or ILs, ion gels can also be endowed with light-responsive functions. As shown in Figure 6A, poly[(2-(4-vinylphenyl)ethene-1,1,2-triyl)-tribenzene-b-ethylene glycol-b-(2- (4-vinylphenyl)ethene-1,1,2-triyl)-tribenzene] [P(TPEE-b-EG-b-TPEE)], which has aggregation-induced emission (AIE), is synthesized.[73] Ion gels with UV response can be prepared by mixing them in physically, and their fluorescence wavelength is 480 nm (blue light). With further introduction of the luminescent metal ion Eu^{3+}, the ion

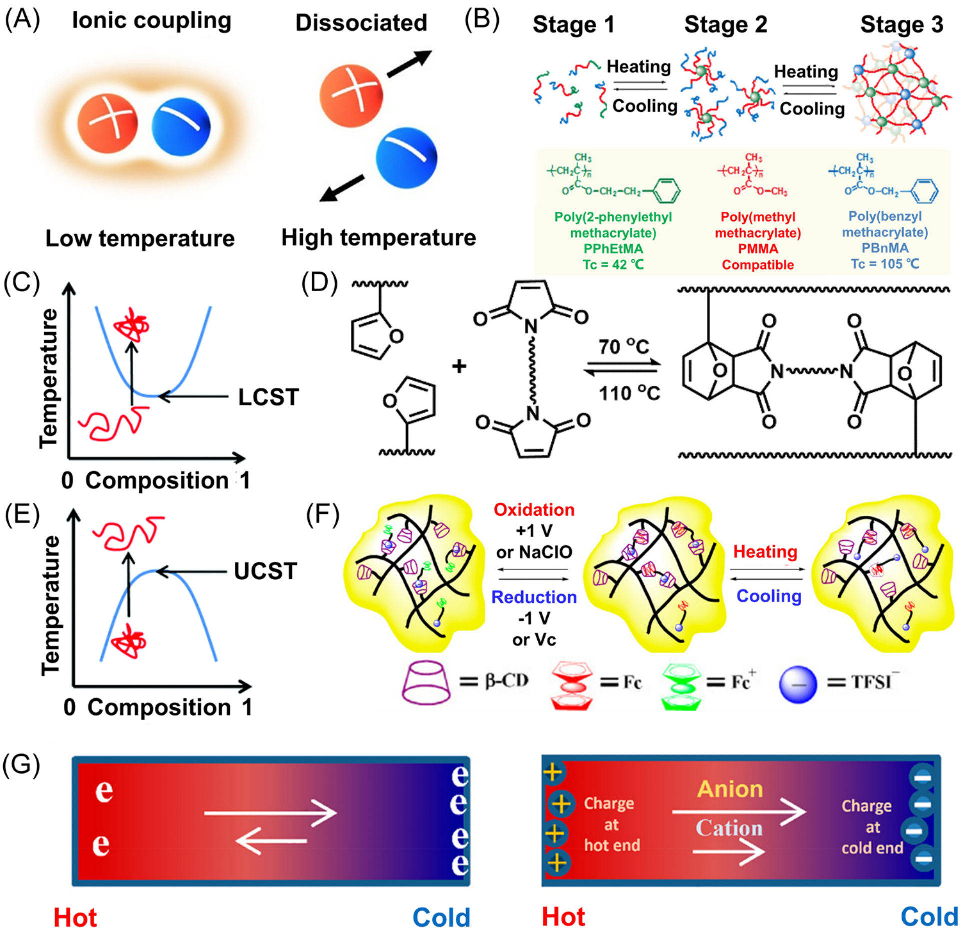

FIGURE 5 (A) Mechanism of the influence of temperature on the ion pair decoupling–coupling. Reproduced with permission: Copyright 2020, American Chemical Society.[66] (B) Scheme of the sol–gel process. Reproduced with permission: Copyright 2016, American Chemical Society.[67] (C) Illustration of the lower critical solution temperature (LCST). Reproduced under the terms of the Creative Commons Attribution 3.0 Unported license: Copyright 2015, Royal Society of Chemistry.[68] (D) Mechanism of the influence of temperature on the dynamic covalent bonds. Reproduced with permission: Copyright 2018, American Chemical Society.[69] (E) Illustration of the upper critical solution temperature (UCST). Reproduced with permission: Copyright 2015, Royal Society of Chemistry.[68] (F) Temperature response of the supramolecular ion gels. Reproduced with permission: Copyright 2014, American Chemical Society.[70] (G) Illustration of the Soret effect. Reproduced with permission: Copyright 2022, American Chemical Society.[71]

gels can be excited to fluorescence at 615 nm (red light) under UV light. By adjusting the ratio of the two fluorescent components, the fluorescence wavelength can be freely adjusted in the range of blue to red light (Figure 6B). Besides polymer-based ion gels, light response can also be achieved by introducing photothermal substances with photothermal conversion capabilities into ion gels (Figure 6C).[74] For example, by covalently attaching a pyrrole molecule with near-infrared light response to the imidazole cation of an IL, a one-step oxidative polymerization can yield PILs that can respond to near-infrared light.[75] Unlike the fluorescence indication of the above-mentioned ion gels, PILs have a narrower energy band and are capable of converting near-infrared light into heat through photothermal conversion and further enhancing the ionic conductivity of the poly(ILs) (Figure 6D). The use of an inorganic nano-ion composite of ionic gels is the third method to achieve photo response. Due to the good dispersion of carbon nanotubes in ILs and the high photothermal conversion efficiency of carbon nanotubes, a photothermal IL with a carbon tube composite can be easily obtained by using the preparation process of inorganic ion gels (Figure 6E,F).

3.2 | Chemical signals

Most ILs contain quaternary ammonium structures and are sensitive to gas molecules such as carbon dioxide, ammonia, and hydrogen sulfide. For example, Wöllenstein and colleagues[76] prepared carbon dioxide-responsive ion gels using metal oxides, polymers, ILs, and so on. Tanaka et al.[77] determined the effect of hydrogen, ammonia, and ethanol on the bilayer at the ion gel/metal electrode interface and identified and screened the gas mixture on the basis of

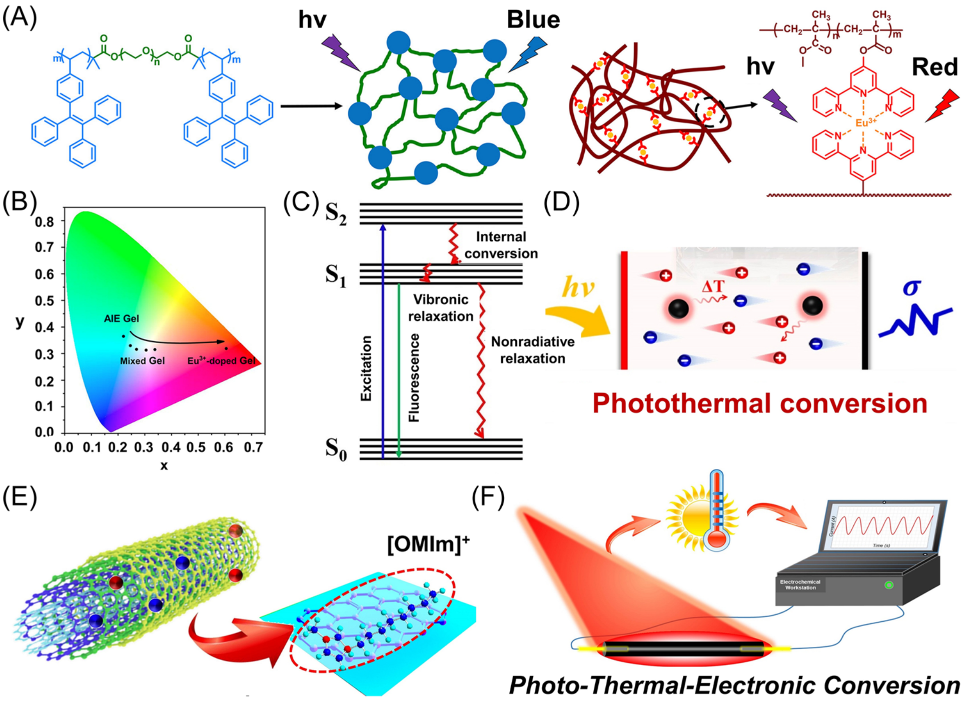

FIGURE 6 (A) Polymer skeleton modified with light-emitting groups. (B) Modulation of the luminescence spectrum by the mixing ratio of luminescent groups. Reproduced with permission: Copyright 2020, American Chemical Society.[73] (C) Mechanism of photo-thermal conversion. Reproduced with permission: Copyright 2022, Wiley-VCH.[74] (D) Mechanism of light-responsive PILs. Reproduced with permission: Copyright 2019, American Chemical Society.[75] (E) Interaction between the carbon nanotubes and the ILs.[74] (F) Illustration of ion gels' photo-thermal conversion. Reproduced with permission: Copyright 2022, Wiley-VCH.[74]

changes in the signal of the interfacial bilayer. When the interface responds to the gas, the interfacial bilayer is altered so that a weak voltage signal is output.

Using the pH regulation of intermolecular interactions, changes in the pH environment can alter the optical, electrical, or mechanical properties of ion gels. As shown in Figure 7A, Baker and colleagues[78] prepared pH-sensitive fluorescent ILs by designing the pH-responsive fluorescent group 8-hydroxypyrene-1,3,6-trisulfonate (HPTS, pyranine) as the anion of the ILs. Due to the pH sensitivity of this IL, it also showed good response to alkaline gas molecules such as ammonia (Figure 7B). Yan and colleagues[79] prepared a series of pH-responsive ion gels by introducing cresol red (CR), methyl orange (MO), and bromothymol blue (TB) molecules into ion gels using an anion exchange process (Figure 7C). Taking PIL-CR as an example, the absorption spectrum of the ion gel can be red-shifted to a certain extent at pH > 7 due to the exchange of hydroxide ions (Figure 7D). pH-responsive ion gels can be achieved by modifying MIPIL and bovine serum albumin (BSA) onto the surface of 3-aminopropyl triethoxysilane-modified MWCNTs (MWCNTs@BSA-MIPILs) (Figure 7E).[80] The binding energy between MWCNTs-MIPILs and BSA can be tuned by adjusting the pH. For instance, on increasing the pH from 7.7 to 9.9, the impacting factors increased from 1.30 to 5.06. Wu and colleagues[82] prepared pH-responsive electrodes based on the THF solution of n-cetylpyridinium hexafluorophosphate (CPFP), poly(vinyl chloride) (PVC), and quinhydrone (QH). The following electrode reaction equilibrium equation occurs at the QH electrode:

$$C_6H_4O_2 + 2H^+ + 2e^- \rightarrow C_6H_4(OH)_2.$$

From the reaction equation, it is clear that the solution pH can alter the electrode potential of the ion gel electrode, which results in a pH-responsive ion gel. Guirado and colleagues[81] assembled nitrospiropyran-doped ion gels with a multiresponsive performance, such as photo, pH, thermal, and electrochromic switching behaviors (Figure 7F). Herein, the pH responsiveness is mainly attributed to the reversible transition of the protonated state on changing the pH environment. On adding the base, a new absorption band appears at 303 nm due to the formation of protonated merocyanine isomers.

4 | EMERGING APPLICATIONS

4.1 | Ionic tactile sensors

The ion transport mechanism of ion gels is theoretically more compatible with various biological signals, thus

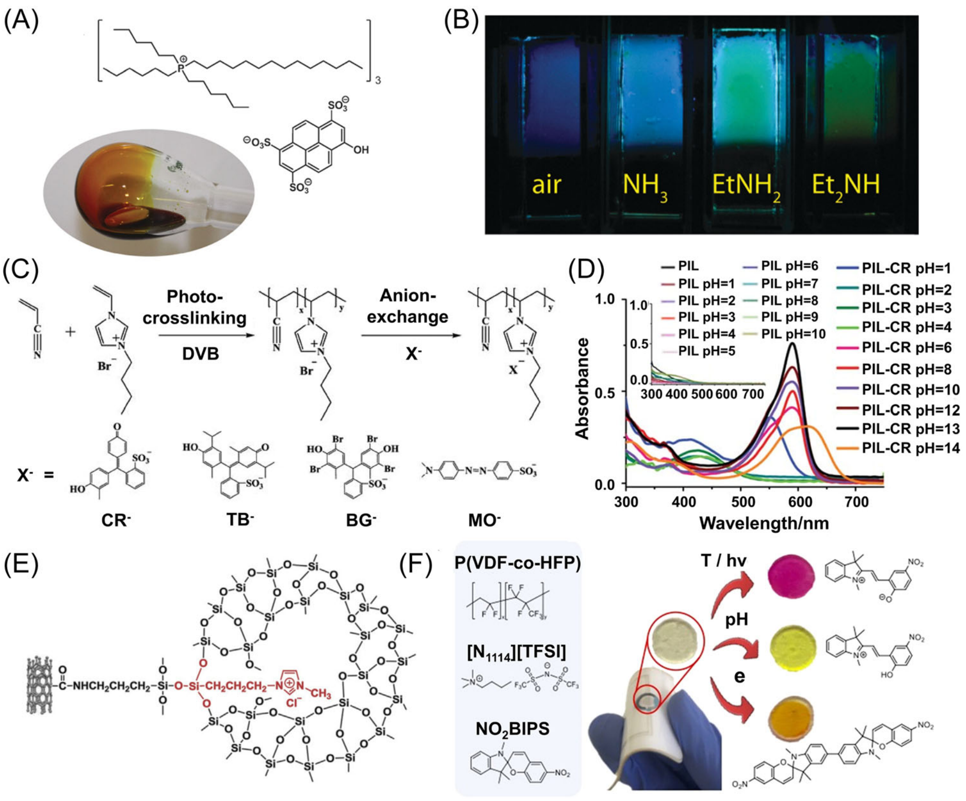

FIGURE 7 (A) Structure of pH-responsive ILs. (B) pH response of ILs in different environments. Reproduced with permission: Copyright 1996, Royal Society of Chemistry.[78] (C) Synthesis process of pH-responsive PILs. (D) Absorption spectra of PIL-CR in different pH environments. Reproduced with permission: Copyright 2010, Royal Society of Chemistry.[79] (E) Structure of pH-responsive MWCNTs@BSA-MIPILs. Reproduced with permission: Copyright 2016, Elsevier B.V.[80] (F) EMF signals of pH-responsive ion gels in different pH environments. Reproduced under the terms of the Creative Commons Attribution 3.0 Unported license: Copyright 2023, American Chemical Society.[81]

making ion gels one of the most important materials in the field of haptic sensing.[83] Two special signals are more important in the field of haptic sensing: the temperature signal and the pressure signal.

We have already discussed the temperature response mechanisms of ion gels in the above chapter. The sensing mechanism mostly used in ionic temperature sensors is the temperature effect of ion pair decoupling–coupling. Compared to other sensing mechanisms, this response mechanism can establish the physical relationship between temperature and ionic conductivity more accurately. Yamada and Toshiyoshi[66] prepared temperature-responsive ion gels based on PVA and tris(2-hydroxy-ethyl) methylammonium ethylsulfate ($[MTEOA]^+[MeOSO_3]^-$), which can respond electrically to temperature based on the ion-pair decoupling–coupling mechanism (Figure 8A). The relative conductivity change of the sensor was about 1200% when the temperature was increased from 30°C to 80°C (Figure 8B).[66] Wang and colleagues[84] developed electronic tattoo patches for temperature monitoring based on dynamic ion gels (Figure 8C). The tattoo patch is capable of reversible writing and erasing as the ion gel has a temperature-responsive dynamic IL 1-ethyl-3-methylimidazolium thioctate ([EMIm][TA]). Most importantly, the PILs with dynamic covalent bonding include both the temperature effect of ion-pair decoupling–coupling and temperature-responsive dynamic covalent bonding mechanisms, which further enhances the sensitivity of temperature response in this kind of ion gel. As shown in Figure 8D, the relative conductivity of this ion gel can change up to 150% when the temperature is increased from 25°C to 40°C. Another crystal-limited ion gel was also developed for the preparation of ionic temperature sensors. Wang and colleagues[61] synthesized an IL crystal consisting of an anion with an azo phenyl group and an imidazolium cation. The melting point of this IL crystal is very low (70°C). The IL crystal is capable of stacking in an orderly manner between the benzene ring and the benzene ring, the benzene ring and the imidazole ring, and the imidazole ring and the imidazole ring. This can confine the conventional IL in the IL crystal and form a supramolecular ion gel. A temperature sensor prepared from this supramolecular ion gel can achieve a very sensitive temperature response. The relative conductivity of the ion gel can change up to 900% when the temperature increases from 25°C to 60°C. Soret effect-based ionic thermoelectric devices can also be used as temperature-responsive iontophoresis sensors. This has been

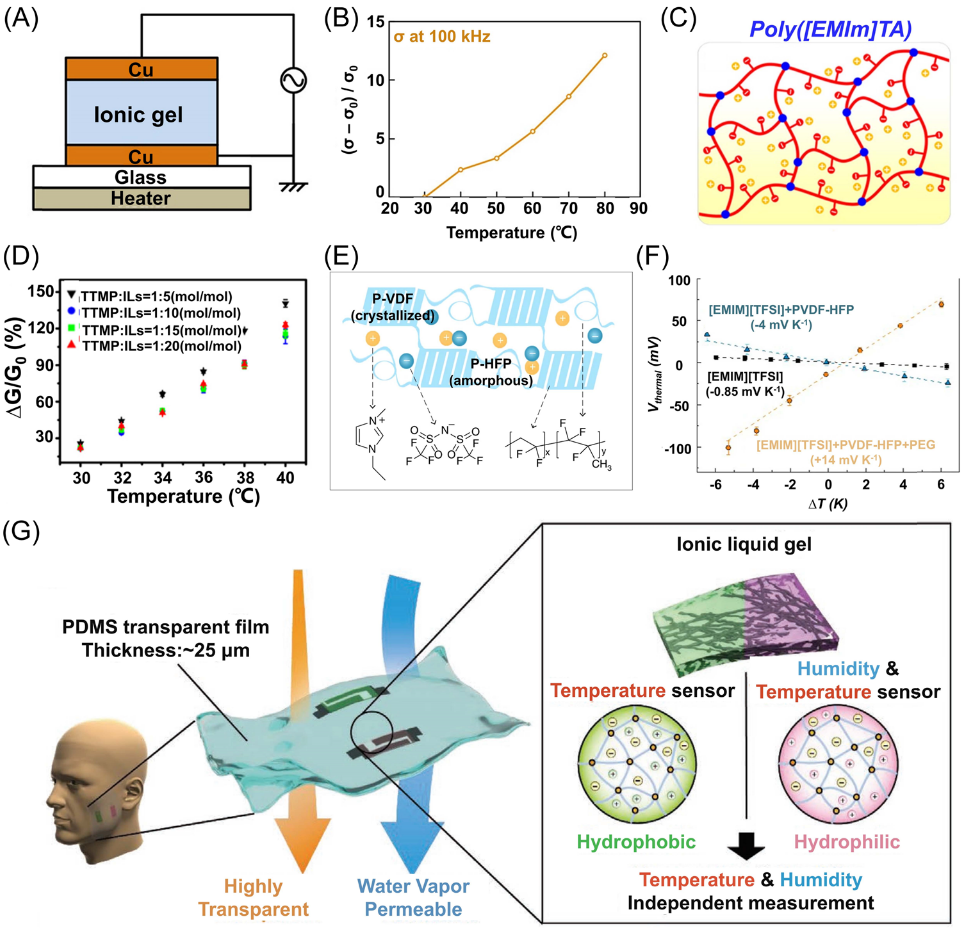

FIGURE 8 (A) Illustration of the ionic temperature sensor.[66] (B) Relative conductivity changes of the ionic temperature sensor at different temperatures. Reproduced with permission: Copyright 2020, American Chemical Society.[66] (C) Structure of PILs with dynamic covalent bonds.[84] (D) Relative conductivity changes of dynamic PILs at different temperatures. Reproduced with permission: Copyright 2021, American Chemical Society.[84] (E) Structure of the ion gels with thermal-electric conversion.[85] (F) Seeback coefficient of ion gels with different components. Reproduced under the terms of the Creative Commons CC BY license: Copyright 2019, Springer Nature.[85] (G) Illustration of temperature–humidity dual-mode ionic sensors. Reproduced with permission: Copyright 2022, Wiley-VCH.[86]

demonstrated in many studies. Zhao et al.[85] designed a bipolar ion gel based on the thermoelectric effect that can respond to the temperature (Figure 8E). The higher the Seeback coefficient of the ion gel, the higher the sensitivity of its temperature sensor. The results show that the Seeback coefficient of ion gels can be adjusted on the basis of the components of ion gels. As shown in Figure 8F, [EMIm][TFSI] has a negative Seeback coefficient (−0.85 mV/K). On blending [EMIm][TFSI] with PVDF-HFP, the Seeback coefficient can be increased to −4.00 mV/K. Further, after the introduction of PEG, the ion gel shows a positive Seeback coefficient (14.0 mV/K). This is mainly due to the fact that PEG is more favorable for the migration of imidazolium cations. The temperature sensing performance of the ion gels is also often affected by humidity conditions because they tend to absorb moisture from the air. To address the influence of humidity on temperature sensing, Isano et al.[86] prepared hydrophobic ion gels using trihexyltetradecylphosphonium bis(trifluoromethanesulfonyl)amide ($[P_{6,6,6,14}]$[TFSA]) and poly(vinylidene fluoride-co-hexafluoropropylene) (PVDF-HFP). The ion gels were able to respond effectively and specifically to temperature signals. In addition, Isano et al. further prepared ionic gels that responded to both temperature and humidity using tetraglyme and lithium bis-(trifluoromethanesulfonyl) amide ([Li(G4)][TFSA]) and a polyether–polyamide thermoplastic elastomer (Pebax MH1657), and used the signal resolution of the above two gels for accurate analysis of temperature and humidity signals (Figure 8G).

The design of micro–nano structures of pressure sensors has a major effect on the sensitivity, linearity, and response range of the sensors. Recent ionic pressure sensors have introduced many micro–nano structures. As shown in Figure 9A, Niu et al.[87] completely mimicked the skin structure based on ion gels at various levels, namely, the epithelial tissue and hair (PDMS and LMS PDMS/Au), the epidermis (double-sided LMS and PVDF-HFP/[EMIM][TFSI]), and the dermis (single-sided LMS Au/PDMS). The

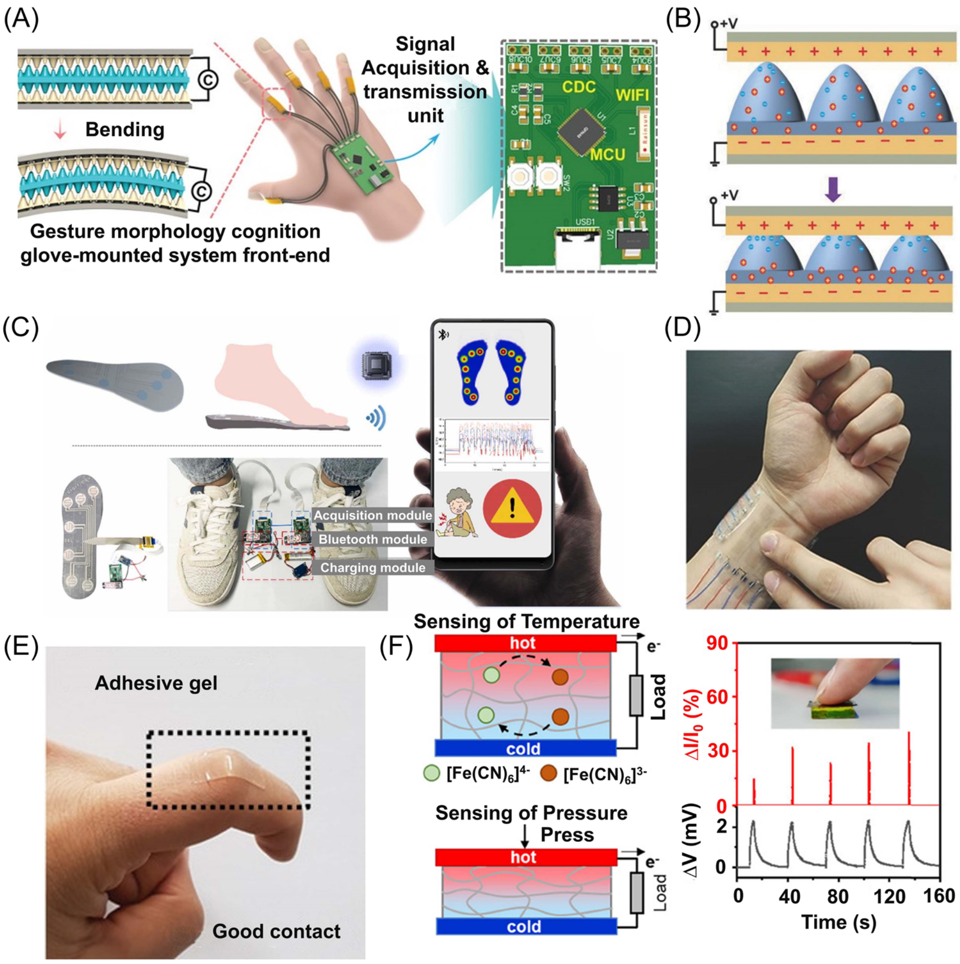

FIGURE 9 (A) Scheme of ionic sensors that mimic the complete structures of the skin and a wireless transmit system. Reproduced with permission: Copyright 2022, Wiley-VCH.[87] (B) Response mechanism of ionic pressure with micro-structures. Reproduced with permission: Copyright 2018, Wiley-VCH.[88] (C) Illustration of the detecting system of feet. Reproduced with permission: Copyright 2022, Elsevier Ltd.[89] (D) Photograph of the ionic sensor arrays. Reproduced with permission: Copyright 2016, Wiley-VCH.[90] (E) Display of highly adhesive ion gels. Reproduced with permission: Copyright 2021, Wiley-VCH.[91] (F) Measurement of temperature-pressure dual-mode ionic sensors. Reproduced with permission: Copyright 2022, American Chemical Society.[92]

fully skin-simulated sensor has ultrahigh sensitivity (8053.1 kPa^{-1} in the range of ~1 kPa), high linear sensitivity (3103.5 kPa^{-1} in the range of 1–34 kPa), and a fast response time. The fully skin-analog sensor can be integrated with a microcontroller and a wireless transmission device to enable real-time monitoring of hand movements. Thanks to the multistage microstructure inside the leaf, the sensor has a very sensitive response (over 1 kPa^{-1}) in the pressure range from as low as 0.1 Pa to as high as 115 kPa (Figure 9B).[88] Finite element analysis was also used to analyze the morphology of the ionic pressure sensor based on the micro–nano structure under pressure. Li et al.[89] developed an ion gel-based pressure sensor array by simulating the skin function (Figure 9C). The pressure sensor array can be connected to monitoring and wireless transmission devices for stress analysis of various parts of the foot, allowing further real-time monitoring of gait and a body's condition. As shown in Figure 9D, a sensing array of nano-friction generators was prepared.[90] The array is capable of arrayed motion monitoring of the wrist area. In the above detection devices, it is intuitively important that the ion gel adheres closely to the skin. If the adhesion strength of the device is not sufficient during arm or joint movements, the device will detach from the skin surface, thus affecting the accuracy and precision of the measurements. In Figure 9E, Cho et al.[91] prepared ion gels with high adhesion strength, which were compounded from ILs and poly(tertbutyl styrene-block-(4-hydroxystyrene-random-methyl acrylate)) [poly (tBS-b-(4HS-r-MA)) or PSHM] and poly(tert-butyl styreneblock-(2-vinyl pyridine-random-methyl acrylate)) [poly(tBS-b-(2VP-r-MA)) or PSVM]). Lu et al.[93] further integrated ionic temperature devices and ionic pressure devices to design MXene-based ion gels that can respond to both temperature and pressure. Composite sensors did not show the coupling problem caused by the different signals. Fu et al.[92] proposed thermogalvanic-based gels with good stretchability, selfpower, and temperature-pressure dual-mode responsibilities (Figure 9F). The thermocouple gel has an equivalent Seebeck coefficient of −1.21 mV/K and a pressure sensitivity of 0.056 kPa^{-1}. Recently, Bao and colleagues[94] published a paper in *Science* titled "Artificial multimodal receptors based on ion relaxation dynamics" that explores the role of ion relaxation effects on the decoupling of temperature and strain in ionic devices. This will provide some ideas for the design of ion gel devices with decoupled temperature and strain.

4.2 | Ion-gated transistors

An interfacial double layer exists at the interface between ion gels and metals or semiconductors. The presence of the interfacial capacitance of the ion gel can significantly reduce the turn-on voltage of the transistor compared to a conventional transistor with insulating dielectrics. Therefore, ion gels are favored by researchers in the field of low-power and low-voltage transistors. In addition, flexible and highly stretchable ion gels can also be used for the preparation of flexible and stretchable transistors. In Figure 10A, a thin-film transistor also has some stretchability due to the use of PDMS and ion gels.[95] Most importantly, the nanoscale phase separation within the ion gel reduces the switching time of the transistor to less than 20 μs (Figure 10B). As shown in Figure 10C, Oh et al.[96] constructed a bipolar transistor based on a bipolar graphene/pentacene structure by using an ion gel as the gate. Ren et al.[97] studied the carrier migration of a transistor with an ionic gate using cryogenic microwave impedance microscopy (MIM) and established the first electron-realistic spatial image of the channel conductance (Figure 10D). The modulation of graphene plasma effects by

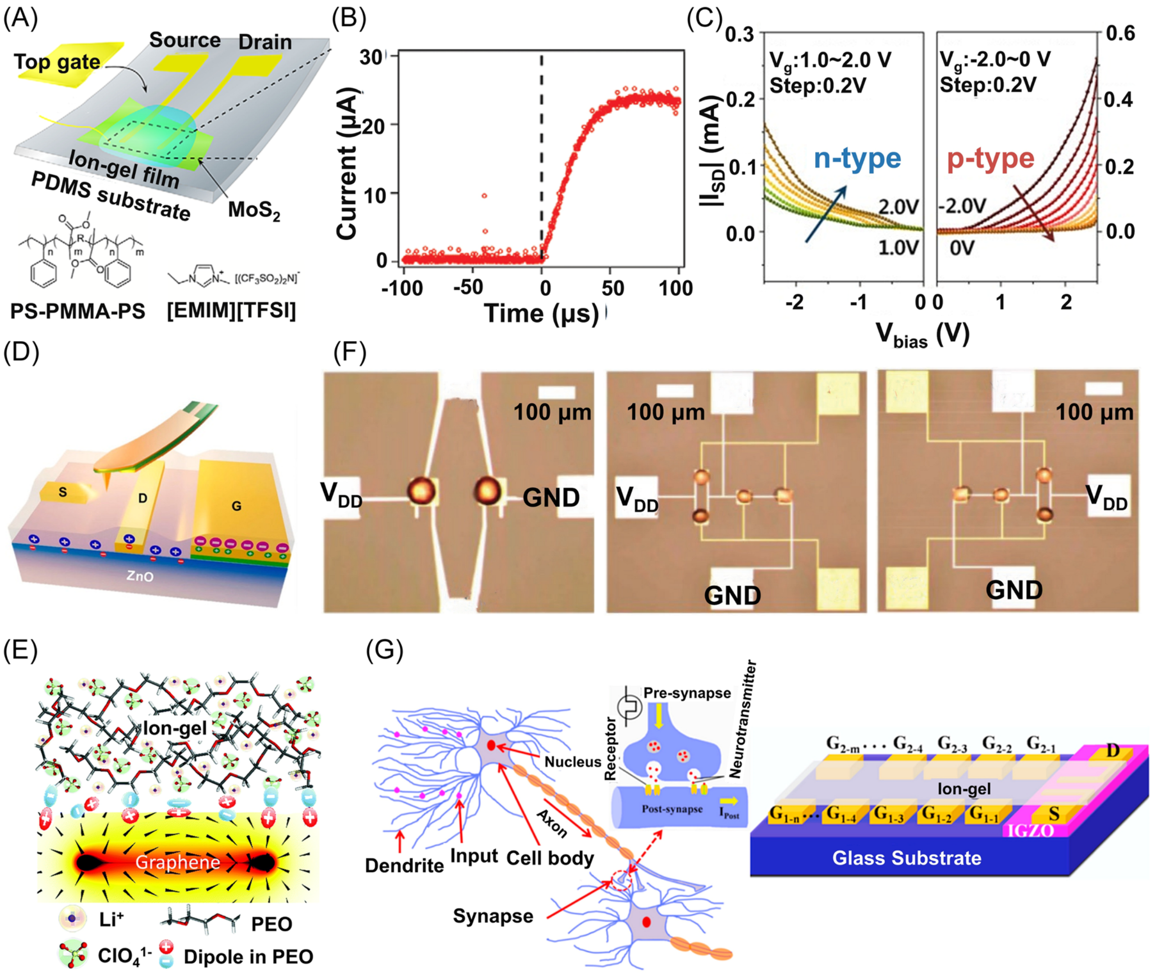

FIGURE 10 (A) Structure of ion-gated transistors. (B) Response time of the ion-gated transistor. Reproduced with permission: Copyright 2013, AIP Publishing.[95] (C) Transfer characteristic curve of an ion-gated bipolar transistor. Reproduced with permission: Copyright 2015, American Chemical Society.[96] (D) Illustration of cryogenic microwave impedance microscopy used for the imaging display of carrier movement. Reproduced with permission: Copyright 2015, American Chemical Society.[97] (E) Scheme of the impact of ion gels on the plasmonic effect of graphene. Reproduced with permission: Copyright 2015, Royal Society of Chemistry.[98] (F) Illustration of the ionic logic devices. Reproduced with permission: Copyright 2018, Wiley-VCH.[99] (G) Structure of the neuron-mimicking ion-gated transistors. Reproduced with permission: Copyright 2017, Elsevier B.V.[100]

ion gels has also been studied. In Figure 10E, Hu et al.[98] prepared a field-effect transistor of graphene, using ion gels as gates. It was found that the field-effect transistor was able to achieve a width-tunable graphene plasmon effect (1270 cm^{-1}) at a low-voltage modulation (4 V). Ionic gels have not only been used to assemble single transistors but also logic devices and neural devices based on ionic gels have been investigated (Figure 10F).[99] This greatly enhances the application prospects of ion-gate transistors. Moreover, such ionic logic devices are further used in spatially relevant neuronal circuits. Sun and colleagues[100] designed an artificial neural device by simulating the structure of a neuro synapse as shown in Figure 10G. This artificial neural device uses indium tin oxide as the semiconductor layer and ionic gel as the insulating layer. To simulate this function, an artificial neural device is also designed with an array of gates for collecting stimulation signals at different locations. This opens a new path for the application of ion gels in the field of neural computing.

4.3 | Artificial muscle

Muscles play a crucial role in human movement. Similarly, artificial muscles are also capable of achieving braking behavior under electrical signal stimulation, thus providing electric field-controlled traction for machines as well as artificial exoskeletons. The structure of a typical artificial muscle is shown in Figure 11A.[101] Metal electrodes are machined on the surface of each side of the ion gel, forming a metal–ion gel–metal sandwich structure. As shown in Figure 11B, when a voltage is applied to both sides of the metal electrodes, the anions and cations inside the ion gel move toward the positive and negative electrodes of the metal electrodes, respectively.[50] Due to the difference in the volume and migration rate of anions and cations, the ion concentrations on both sides of the ion gel differ, resulting in asymmetric swelling on both sides of the ion gel. This means that either the positive region swells more than the negative region, or the opposite occurs. This asymmetric swelling behavior allows the ion gel to undergo positive or negative bending, thus achieving the braking behavior of the ion gel. Ion gels based on polyvinyl chloride (PVC), dibutyl adipate (DBA), and 1-allyl-3-methylimidazolium bis((trifluoromethyl) sulfonyl) imide ([AMIM][TFSI]) were prepared by Liang and colleagues[102] The ion gels were further used to assemble fast-responding artificial muscles. According to Figure 11C, the PVC/DBA gel and PVC/DBA/IL gels with different ILs have response times for electric field responses and recovery of about 4.5 and 6 s, respectively. For instance, when the voltage is increased from 6.4 kV to zero within 1 s, the displacement takes 4.3 s for the PVC/

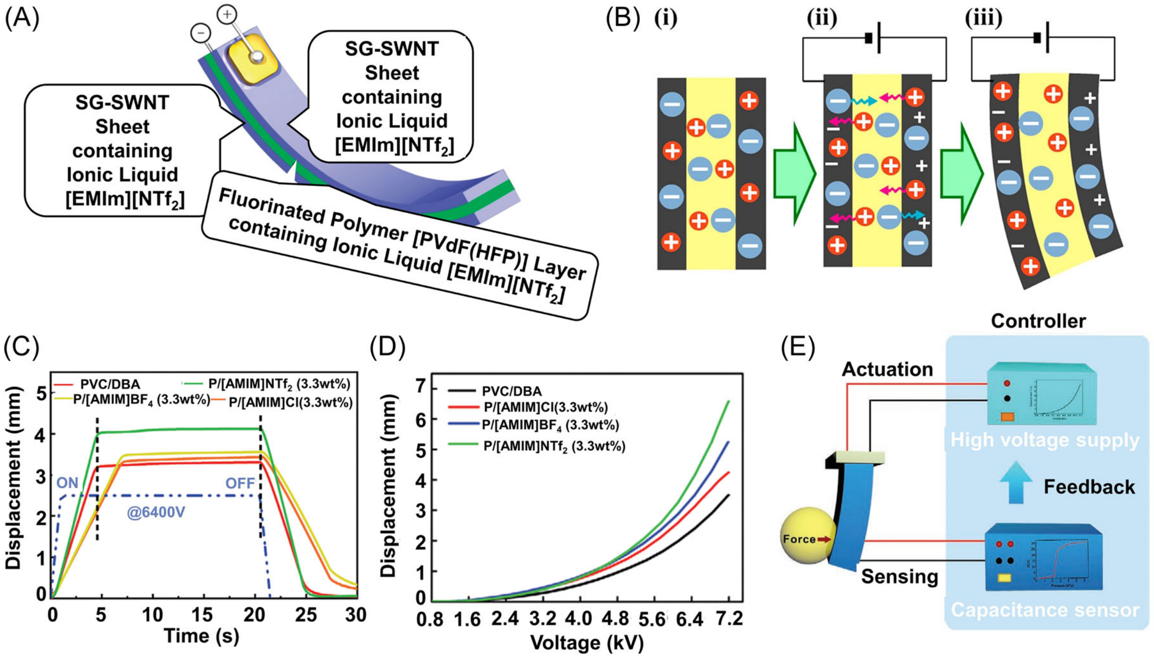

FIGURE 11 (A) Illustration of the structure of ionic artificial muscles. Reproduced with permission: Copyright 2011, Royal Society of Chemistry.[101] (B) Electroactive mechanism of ion gels. Reproduced with permission: Copyright 2018, Elsevier Ltd.[50] (C) Response time of ionic artificial muscles.[102] (D) Effect of the content of ILs on the displacement of the ionic artificial muscles.[102] (E) Feedback process of the ionic artificial muscles. Reproduced with permission: Copyright 2022, Wiley-VCH.[102]

DBA gel and 4.7 s for the P/[AMIM]NTF2 (3.3 wt%) gel to stabilize. The recovery time of bending displacement for the P/[AMIM]NTF2 (3.3 wt%) gel is also comparable to the PVC/DBA gel (6 s) on decreasing the voltage. As shown in Figure 11D, this electrically driven property of ion gels can be changed by adjusting the concentration of ions in the ion gel. In addition, the artificial muscle can also show certain ionic piezoelectric properties when an external force is applied to it (Figure 11E). Due to this, the artificial muscle has both sensor and brake functions, which provides the possibility of subsequent feedback manipulation of the artificial muscle.

4.4 | Display device

Electrochromic ion gels have important applications in the fields of information storage, imaging, and display.[10] In general, conventional ion gels do not possess electrochromic capabilities. Electrochromic ion gels often need to contain electrochromic light-emitting groups. For example, the conductive polymer poly(viologen) can undergo a redox reaction in the presence of an electric field (Figure 12A).[103] The absorption peaks of its redox products are shifted, resulting in a change in the color of the polymer. Moreover, the electrochromic behavior of poly(viologen) can be

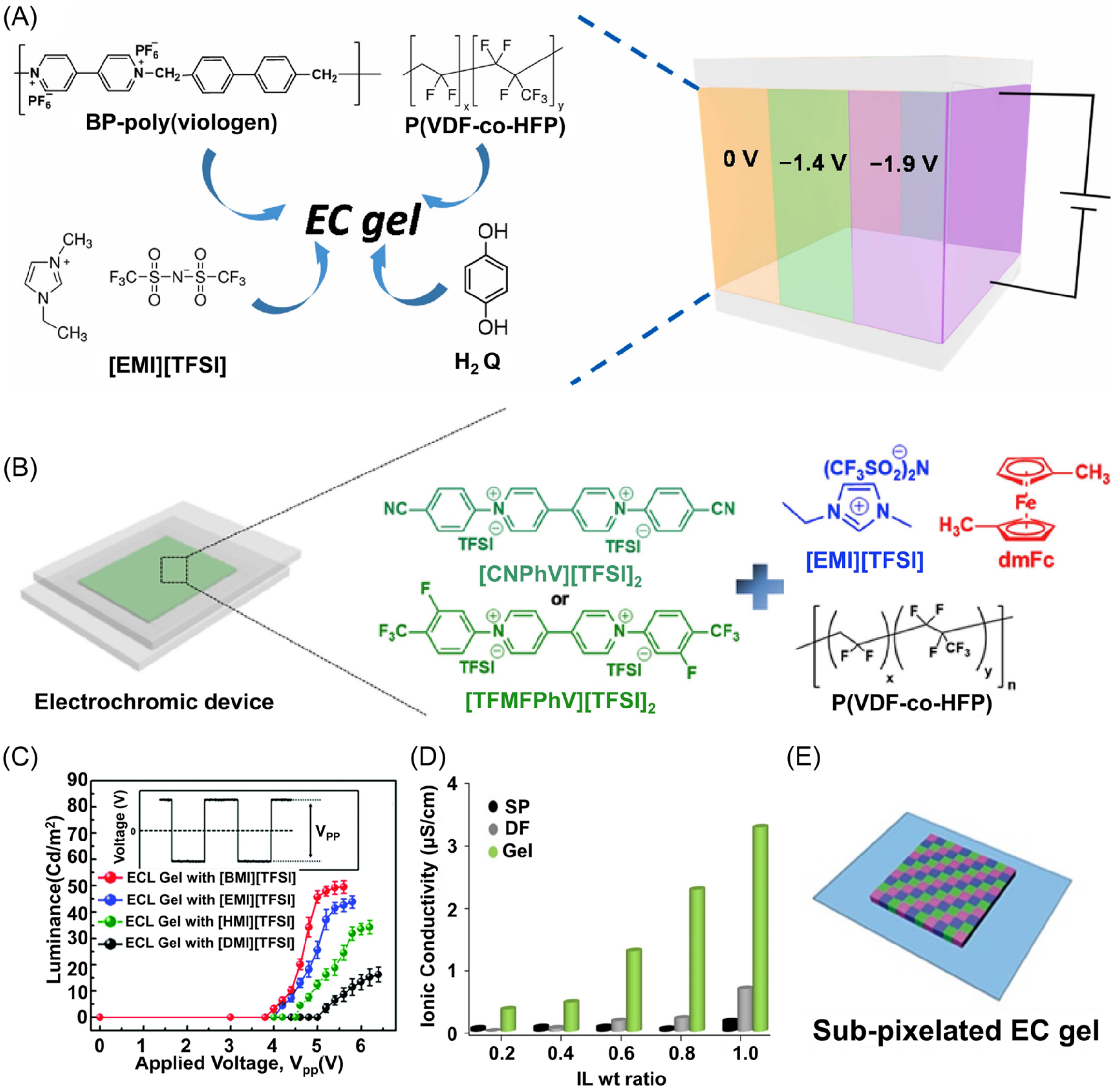

FIGURE 12 (A) Structure of electrochromic ion gels based on the BP-poly(viologen). Reproduced with permission: Copyright 2021, Elsevier B.V.[103] (B) Structure of electrochromic ion gels based on the TFMFPhV^{2+}. Reproduced with permission: Copyright 2017, Elsevier B. V.[104] (C) Influence of the cation of ILs on the luminance of electrochromic ion gels. Reproduced with permission: Copyright 2016, Royal Society of Chemistry.[105] (D) Influence of the contents of ILs on the luminance of electrochromic ion gels. Reproduced with permission: Copyright 2020, American Chemical Society.[106] (E) Illustration of sub-pixelated electrochromic ion gels. Reproduced with permission: Copyright 2019, Wiley-VCH.[107]

modulated by adjusting the N-substituents and molecular weight. Kim and colleagues[103] developed a new class of electrochromic polymers BP-poly(viologen) based on biphenyl and viologen and assembled electrochromic ion gels based on this polymer. Among them, the reducing component is hydroquinone (H_2Q). When the voltage was reduced from 0 to −1.4 V, BP-poly(viologen)$^{2+}$ was reduced to green BP-poly(viologen)$^{+\cdot}$. The absorption peak of the ionic gel shifted to 617 nm. As the voltage continued to decrease to −1.9 V, BP-poly(viologen)$^{+\cdot}$ continued to be reduced to the purple-red BP-poly(viologen)^{0} species. At this point, the absorption peak of the ionic gel continued to shift to 534 nm. In Figure 12B, Moon and colleagues[104] synthesized a green viologen^{+} by the zincke reaction of a green viologen derivative (1,1′-bis(3-fluoro-4-(trifluoromethyl) phenyl)-4,4′-bipyridinium (TFMFPhV^{2+}). The electrochromic material is compounded with IL to obtain electrochromic ion gels. Moreover, the operating voltage for the electrochromic ion gel was reduced to 0.23 V. This will help to reduce the power consumption of the ionic electrochromic device and improve the lifetime and safety of the device. As shown in Figure 12C, Frisbie and colleagues[105] investigated the effect of the IL type on an electrochromic ion gel. It was shown that for imidazolium ILs, the shorter the substituent of imidazole cation, the lower the operating voltage of electrochromic ion gels (Figure 12D).[106] Kim and Myoung[107] assembled an arrayed display based on electrochromic ion gels (Figure 12E). This confirms the promising application of electrochromic ion gels in the field of arrayed active displays.

5 | CONCLUSION

In conclusion, functional derivation is reviewed to describe the relationship between the structure and stimulus responsiveness of ion gels. Four synthesis paths of ion gels have been illustrated, which include the polymer-blended method, PILs, supramolecular techniques, and the inorganic-blended method. From the perspective of ionic conductivities, inorganic-blended ion gels have been found to have the highest conductivity among these four patterns. This is mainly because the ionic conductivities of ILs are theoretically the upper limit of the conductivities of ion gels. Also, the ion gels prepared in this way hardly decrease the ionic conductivities of ILs. Despite this, inorganic-blended ion gels have poor mechanical properties that limit their applications in smart electronics. Polymer-blended ion gels do not have this mechanical problem owing to the strong interaction between the polymer chain and ILs. Relatively, the ionic conductivities of polymer-blended ion gels can maintain the level of pure ILs to a high degree. The limitation of polymer-blended ion gels is the phase separation of the polymer skeleton and ILs due to the differences between these two components. PILs and supramolecular ion gels bind the cations or anions to the chain of the polymer, which exacerbates the issue of phase separation. However, at the same time, the ionic conductivities of ion gels will be reduced due to the decease of free ions. Therefore, the selection of the synthesis method should fulfill the practical requirements of the performance of ion gels.

Based on these synthesis methods, functional derivatives can be achieved by connecting corresponding functional groups to the ion gels. Temperature-responsive ion gels can be adjusted by tuning the interactions of ions and polymer skeletons. The decoupling–coupling of ions can respond to the temperature electrically. A system with LCST and UCST can support a slight change to the temperature. As for the pressure response, construction of a highly elastic polymer network will improve the sensitivity and responsiveness of the pressure response. Also, the introduction of photo-responsive, pH-responsive, or electrochromic groups will confer various corresponding functions to the ion gels. These ion gels can be further used to assemble smart electronic devices with varying functions. Previously, we summarized the various mechanisms of intelligent responses. It is important to note that functional structures that can convert stimulus responses into electrical signals are more useful for subsequent assembly of highly sophisticated devices.

The advent of the smart era has greatly contributed to the development of intelligent electronic devices. As one of the keys, ion gels can provide reliable material support for ultra-stretchable flexible electronic devices, neural decision-making devices, low-power logic circuits, and brain-computer interfaces due to their rich tunability of mechanical and electrical properties. However, there are several challenges in the field of ionic devices that need to be addressed. How to balance the mechanical strength and ionic conductivity of ionic gels is still a topic that needs further experimental verification and theoretical analysis. Additionally, the specificity of the ion gel stimulus response in complex environments is also a key impediment to the practical application of ion-based devices. Only after these challenges are resolved can ionic devices be further developed.

ACKNOWLEDGMENTS

The authors are grateful for the support of the National Natural Science Foundation of China (No. 52125205, U20A20166, and 52192614), the National Key R&D Program of China (2021YFB3200302 and 2021YFB3200304), the Natural Science Foundation of Beijing Municipality (Z180011 and 2222088), the Shenzhen Science and

Technology Program (Grant No. KQTD20170810105439418), and the Fundamental Research Funds for the Central Universities.

CONFLICT OF INTEREST STATEMENT

The authors declare no conflict of interest.

DATA AVAILABILITY STATEMENT

All data are provided in the main text.

ORCID

Naiwei Gao http://orcid.org/0000-0002-7684-1231
Caofeng Pan http://orcid.org/0000-0001-6327-9692

REFERENCES

1. Bernèche S, Roux B. Energetics of ion conduction through the K^+ channel. *Nature*. 2001;414:73-77.
2. Dyre JC, Maass P, Roling B, Sidebottom DL. Fundamental questions relating to ion conduction in disordered solids. *Rep Prog Phys*. 2009;72:046501.
3. Sata N, Eberman K, Eberl K, Maier J. Mesoscopic fast ion conduction in nanometre-scale planar heterostructures. *Nature*. 2000;408:946-949.
4. Liu J, Zhang Z, Qiao S, Fu G, Wang S, Pan C. Lateral bipolar photoresistance effect in the CIGS heterojunction and its application in position sensitive detector and memory device. *Sci Bull*. 2020;65:477-485.
5. Ren J, Zhang W, Wang Y, et al. A graphene rheostat for highly durable and stretchable strain sensor. *InfoMat*. 2019;1:396-406.
6. Zhang Q, Zuo S, Chen P, Pan C. Piezotronics in two-dimensional materials. *InfoMat*. 2021;3:987-1007.
7. Delisle BP, Anson BD, Rajamani S, January CT. Biology of cardiac arrhythmias: ion channel protein trafficking. *Circ Res*. 2004;94:1418-1428.
8. Peng D, Liu X, Pan C. Epitaxial lift-off for controllable single-crystalline perovskites. *Sci Bull*. 2021;66:6-8.
9. Wang C, Ma R, Peng D, et al. Mechanoluminescent hybrids from a natural resource for energy-related applications. *InfoMat*. 2021;3:1272-1284.
10. Han X, Xu Z, Wu W, Liu X, Yan P, Pan C. Recent progress in optoelectronic synapses for artificial visual-perception system. *Small Struct*. 2020;1:2000029.
11. Li J, Yuan Z, Han X, et al. Biologically inspired stretchable, multifunctional, and 3D electronic skin by strain visualization and triboelectric pressure sensing. *Small Sci*. 2022;2:2100083.
12. Liu X, Yang X, Gao G, et al. Enhancing photoresponsivity of self-aligned MoS_2 field-effect transistors by piezo-phototronic effect from GaN nanowires. *ACS Nano*. 2016;10:7451-7457.
13. Zhou R, Hu G, Yu R, Pan C, Wang ZL. Piezotronic effect enhanced detection of flammable/toxic gases by ZnO micro/nanowire sensors. *Nano Energy*. 2015;12:588-596.
14. Rogers JA, Someya T, Huang Y. Materials and mechanics for stretchable electronics. *Science*. 2010;327:1603-1607.
15. Chen M, Pan C, Zhang T, Li X, Liang R, Wang ZL. Tuning light emission of a pressure-sensitive silicon/ZnO nanowires heterostructure matrix through piezo-phototronic effects. *ACS Nano*. 2016;10:6074-6079.
16. Zhang F, Liu X, Pan C, Zhu J. Nano-porous anodic aluminium oxide membranes with 6–19 nm pore diameters formed by a low-potential anodizing process. *Nanotechnology*. 2007;18:345302.
17. Hammock ML, Chortos A, Tee BCK, Tok JBH, Bao Z. 25th anniversary article: the evolution of electronic skin (e-skin): a brief history, design considerations, and recent progress. *Adv Mater*. 2013;25:5997-6038.
18. Wang C, Pan C, Wang Z. Electronic skin for closed-loop systems. *ACS Nano*. 2019;13:12287-12293.
19. Sun JY, Keplinger C, Whitesides GM, Suo Z. Ionic skin. *Adv Mater*. 2014;26:7608-7614.
20. Leger J, Berggren M, Carter S. *Iontronics: Ionic Carriers in Organic Electronic Materials and Devices*. CRC Press; 2016.
21. Lin P, Pan C, Wang ZL. Two-dimensional nanomaterials for novel piezotronics and piezophototronics. *Materials Today Nano*. 2018;4:17-31.
22. Ahmad M, Rafi-Ud-Din C, Pan C, Zhu J. Investigation of hydrogen storage capabilities of ZnO-based nanostructures. *J Phys Chem C*. 2010;114:2560-2565.
23. Wen X, Wu W, Pan C, Hu Y, Yang Q, Lin Wang Z. Development and progress in piezotronics. *Nano Energy*. 2015;14:276-295.
24. Li F, Xia Z, Pan C, et al. High Br^- content $CsPb(Cl_yBr_{1-y})_3$ perovskite nanocrystals with strong Mn^{2+} emission through diverse cation/anion exchange engineering. *ACS Appl Mater Interfaces*. 2018;10:11739-11746.
25. Sun J, Wang Y, Guo S, et al. Lateral 2D WSe_2 p–n homojunction formed by efficient charge-carrier-type modulation for high-performance optoelectronics. *Adv Mater*. 2020;32:1906499.
26. Dong L, Niu S, Pan C, Yu R, Zhang Y, Wang ZL. Piezo-phototronic effect of CdSe nanowires. *Adv Mater*. 2012;24:5470-5475.
27. Zhou X, Zhao F, Guo Y, Zhang Y, Yu G. A hydrogel-based antifouling solar evaporator for highly efficient water desalination. *Energy Environ Sci*. 2018;11:1985-1992.
28. Lee KH, Kang MS, Zhang S, Gu Y, Lodge TP, Frisbie CD. "Cut and stick" rubbery ion gels as high capacitance gate dielectrics. *Adv Mater*. 2012;24:4457-4462.
29. Xu L, Huang Z, Deng Z, et al. A transparent, highly stretchable, solvent-resistant, recyclable multifunctional ionogel with underwater self-healing and adhesion for reliable strain sensors. *Adv Mater*. 2021;33:2105306.
30. Gao N, Wu X, He Y, Ma Q, Wang Y. Reconfigurable and recyclable circuits based on liquid passive components. *Adv Electron Mater*. 2020;6:1901388.
31. Xiao K, Wan C, Jiang L, Chen X, Antonietti M. Bioinspired ionic sensory systems: the successor of electronics. *Adv Mater*. 2020;32:2000218.
32. Amoli V, Kim JS, Kim SY, et al. Ionic tactile sensors for emerging human-interactive technologies: a review of recent progress. *Adv Funct Mater*. 2020;30:1904532.
33. Li R, Wang L, Kong D, Yin L. Recent progress on biodegradable materials and transient electronics. *Bioactive Mater*. 2018;3:322-333.

34. Wang H, Wang Z, Yang J, Xu C, Zhang Q, Peng Z. Ionic gels and their applications in stretchable electronics. *Macromol Rapid Commun*. 2018;39:1800246.
35. Kim YM, Moon HC. Ionoskins: nonvolatile, highly transparent, ultrastretchable ionic sensory platforms for wearable electronics. *Adv Funct Mater*. 2020;30:1907290.
36. Zhang X, Cui C, Chen S, et al. Adhesive ionohydrogels based on ionic liquid/water binary solvents with freezing tolerance for flexible ionotronic devices. *Chem Mater*. 2022;34:1065-1077.
37. Shalu I, Chaurasia SK, Singh RK, Chandra S. Thermal stability, complexing behavior, and ionic transport of polymeric gel membranes based on polymer PVdF-HFP and ionic liquid, [BMIM][BF4]. *J Phys Chem B*. 2013;117:897-906.
38. Takeno H, Inoguchi H, Hsieh W-C. Mechanically robust ionic liquid gels composed of cellulose nanofiber and poly (vinyl alcohol). *Mater Today Commun*. 2022;31:103495.
39. Lu J, Yan F, Texter J. Advanced applications of ionic liquids in polymer science. *Prog Polym Sci*. 2009;34:431-448.
40. Klingshirn MA, Spear SK, Subramanian R, Holbrey JD, Huddleston JG, Rogers RD. Gelation of ionic liquids using a cross-linked poly(ethylene glycol) gel matrix. *Chem Mater*. 2004;16:3091-3097.
41. Rawat K, Aswal VK, Bohidar HB. DNA–gelatin complex coacervation, UCST and first-order phase transition of coacervate to anisotropic ion gel in 1-methyl-3-octylimidazolium chloride ionic liquid solutions. *J Phys Chem B*. 2012;116:14805-14816.
42. Li T, Wang Y, Li S, Liu X, Sun J. Mechanically robust, elastic, and healable ionogels for highly sensitive ultra-durable ionic skins. *Adv Mater*. 2020;32:2002706.
43. Zhang X, Kar M, Mendes TC, Wu Y, MacFarlane DR. Supported ionic liquid gel membrane electrolytes for flexible supercapacitors. *Adv Energy Mater*. 2018;8:1702702.
44. Pandey GP, Rastogi AC, Westgate CR. Polyacrylonitrile and 1-ethyl-3-methylimidazolium thiocyanate based gel polymer electrolyte for solid-state supercapacitors with graphene electrodes. *ECS Trans*. 2013;50:145-151.
45. Qin H, Owyeung RE, Sonkusale SR, Panzer MJ. Highly stretchable and nonvolatile gelatin-supported deep eutectic solvent gel electrolyte-based ionic skins for strain and pressure sensing. *J Mater Chem C*. 2019;7:601-608.
46. AnkitTiwari, S, Tiwari N, Ho F, et al. High-*k*, ultrastretchable self-enclosed ionic liquid-elastomer composites for soft robotics and flexible electronics. *ACS Appl Mater Interfaces*. 2020;12:37561-37570.
47. Horowitz AI, Panzer MJ. Poly(dimethylsiloxane)-supported ionogels with a high ionic liquid loading. *Angew Chem*. 2014;126:9938-9941.
48. Jia H, He Y, Zhang X, Du W, Wang Y. Integrating ultra-thermal-sensitive fluids into elastomers for multifunctional flexible sensors. *Adv Electron Mater*. 2015;1:1500029.
49. Zhang J, Chen Z, Zhang Y, Dong S, Chen Y, Zhang S. Poly (ionic liquid)s containing alkoxy chains and bis(trifluoromethanesulfonyl)imide anions as highly adhesive materials. *Adv Mater*. 2021;33:2100962.
50. Kokubo H, Sano R, Murai K, Ishii S, Watanabe M. Ionic polymer actuators using poly(ionic liquid) electrolytes. *Eur Polym J*. 2018;106:266-272.
51. D'Angelo AJ, Panzer MJ. Design of stretchable and self-healing gel electrolytes via fully zwitterionic polymer networks in solvate ionic liquids for Li-based batteries. *Chem Mater*. 2019;31:2913-2922.
52. Ren Y, Guo J, Liu Z, et al. Ionic liquid–based click-ionogels. *Sci Adv*. 2019;5:eaax0648.
53. Mathieu K, Jérôme C, Debuigne A. Macroporous poly(ionic liquid)/ionic liquid gels via CO_2-based emulsion-templating polymerization. *Polym Chem*. 2018;9:428-437.
54. Yuan C, Guo J, Yan F. Shape memory poly(ionic liquid) gels controlled by host–guest interaction with β-cyclodextrin. *Polymer*. 2014;55:3431-3435.
55. Sinawang G, Kobayashi Y, Zheng Y, Takashima Y, Harada A, Yamaguchi H. Preparation of supramolecular ionic liquid gels based on host–guest interactions and their swelling and ionic conductive properties. *Macromolecules*. 2019;52:2932-2938.
56. Staňo R, Košovan P, Tagliabue A, Holm C. Electrostatically cross-linked reversible gels—effects of pH and ionic strength. *Macromolecules*. 2021;54:4769-4781.
57. Rizzo C, Mandoli A, Marullo S, D'Anna F. Ionic liquid gels: supramolecular reaction media for the alcoholysis of anhydrides. *J Org Chem*. 2019;84:6356-6365.
58. Rizzo C, Marullo S, Campodonico PR, et al. Self-sustaining supramolecular ionic liquid gels for dye adsorption. *ACS Sustain Chem Eng*. 2018;6:12453-12462.
59. Zhao D, Zhu Y, Cheng W, et al. A dynamic gel with reversible and tunable topological networks and performances. *Matter*. 2020;2:390-403.
60. Liao H, Liao S, Tao X, Liu C, Wang Y. Intrinsically recyclable and self-healable conductive supramolecular polymers for customizable electronic sensors. *J Mater Chem C*. 2018;6:12992-12999.
61. Gao N, He Y, Tao X, Xu X-Q, Wu X, Wang Y. Crystal-confined freestanding ionic liquids for reconfigurable and repairable electronics. *Nat Commun*. 2019;10:547.
62. Oh K, Lee JY, Lee S-S, Park M, Kim D, Kim H. Highly stretchable dielectric nanocomposites based on single-walled carbon nanotube/ionic liquid gels. *Compos Sci Technol*. 2013;83:40-46.
63. Aprile C, Giacalone F, Gruttadauria M, et al. New ionic liquid-modified silica gels as recyclable materials for L-proline- or H–Pro–Pro–Asp–NH_2-catalyzed aldol reaction. *Green Chem*. 2007;9:1328-1334.
64. Huang T, Tian N, Wu Q, Yan W. Keggin-type polyoxometalate-based ionic liquid gels. *Soft Matter*. 2015;11:4481-4486.
65. Nayeri M, Aronson MT, Bernin D, Chmelka BF, Martinelli A. Surface effects on the structure and mobility of the ionic liquid C_6C_1ImTFSI in silica gels. *Soft Matter*. 2014;10:5618-5627.
66. Yamada S, Toshiyoshi H. Temperature sensor with a water-dissolvable ionic gel for ionic skin. *ACS Appl Mater Interfaces*. 2020;12:36449-36457.
67. Kitazawa Y, Ueki T, McIntosh LD, et al. Hierarchical sol–gel transition induced by thermosensitive self-assembly of an ABC triblock polymer in an ionic liquid. *Macromolecules*. 2016;49:1414-1423.
68. Phillips DJ, Gibson MI. Towards being genuinely smart: 'isothermally-responsive' polymers as versatile, programmable scaffolds for biologically-adaptable materials. *Polym Chem*. 2015;6:1033-1043.
69. Tang Z, Lyu X, Xiao A, Shen Z, Fan X. High-performance double-network ion gels with fast thermal healing

capability via dynamic covalent bonds. *Chem Mater*. 2018;30:7752-7759.

70. Yuan C, Guo J, Tan M, Guo M, Qiu L, Yan F. Multistimuli responsive and electroactive supramolecular gels based on ionic liquid Gemini guest. *ACS Macro Lett*. 2014;3:271-275.
71. Cheng H, Ouyang J. Soret effect of ionic liquid gels for thermoelectric conversion. *J Phys Chem Lett*. 2022;13:10830-10842.
72. Higa M, Yamakawa T. Design and preparation of a novel temperature-responsive ionic gel. *J Phys Chem B*. 2004;108:16703-16707.
73. Tang Z, Lyu X, Luo L, Shen Z, Fan X-H. White-light-emitting AIE/Eu^{3+}-doped ion gel with multistimuli-responsive properties. *ACS Appl Mater Interfaces*. 2020;12:45420-45428.
74. Gao N, Wu X, Ma Y, Li X, Jia J, Wang Y. A sunflower-inspired sun-tracking system directed by an ionic liquid photodetector. *Adv Opt Mater*. 2022;11:2201871.
75. He Y, Xu X-Q, Lv S, Liao H, Wang Y. Dark ionic liquid for flexible optoelectronics. *Langmuir*. 2018;35:1192-1198.
76. Ersoez B, Bauersfeld M-L, Wöllenstein J. Ionogel—based composite material for CO_2 sensing deposited on a chemiresistive transducer. *Proceedings*. 2017;1:314.
77. Tanaka T, Hamanaka Y, Kato T, Uchida K. Simultaneous detection of mixed-gas components by ionic-gel sensors with multiple electrodes. *ACS Sens*. 2022;7:716-721.
78. Yung KY, Schadock-Hewitt AJ, Hunter NP, Bright FV, Baker GA. 'Liquid litmus': chemosensory pH-responsive photonic ionic liquids. *Chem Commun*. 2011;47:4775-4777.
79. Guo J, Qiu L, Deng Z, Yan F. Plastic reusable pH indicator strips: preparation via anion-exchange of poly(ionic liquids) with anionic dyes. *Polym Chem*. 2013;4:1309-1312.
80. Liu M, Pi J, Wang X, et al. A sol-gel derived pH-responsive bovine serum albumin molecularly imprinted poly(ionic liquids) on the surface of multiwall carbon nanotubes. *Anal Chim Acta*. 2016;932:29-40.
81. Santiago S, Giménez-Gómez P, Muñoz-Berbel X, Hernando J, Guirado G. Solid multiresponsive materials based on nitrospiropyran-doped ionogels. *ACS Appl Mater Interfaces*. 2021;13:26461-26471.
82. Ping J, Wang Y, Wu J, Ying Y, Ji F. A novel pH sensing membrane based on an ionic liquid-polymer composite. *Microchim Acta*. 2012;176:229-234.
83. Liu Y, Bao R, Tao J, Li J, Dong M, Pan C. Recent progress in tactile sensors and their applications in intelligent systems. *Sci Bull*. 2020;65:70-88.
84. Chen Z, Gao N, Chu Y, He Y, Wang Y. Ionic network based on dynamic ionic liquids for electronic tattoo application. *ACS Appl Mater Interfaces*. 2021;13:33557-33565.
85. Zhao D, Martinelli A, Willfahrt A, et al. Polymer gels with tunable ionic Seebeck coefficient for ultra-sensitive printed thermopiles. *Nat Commun*. 2019;10:1093.
86. Isano Y, Fujita H, Murakami K, et al. Transparent and breathable ion gel-based sensors toward multimodal sensing ability. *Adv Mater Technol*. 2022;7:2200209.
87. Niu H, Li H, Gao S, et al. Perception-to-cognition tactile sensing based on artificial-intelligence-motivated human full-skin bionic electronic skin. *Adv Mater*. 2022;34:2202622.
88. Qiu Z, Wan Y, Zhou W, et al. Ionic skin with biomimetic dielectric layer templated from calathea zebrine leaf. *Adv Funct Mater*. 2018;28:1802343.
89. Li P, Xie L, Su M, et al. Skin-inspired large area iontronic pressure sensor with ultra-broad range and high sensitivity. *Nano Energy*. 2022;101:107571.
90. Khan U, Kim TH, Ryu H, Seung W, Kim SW. Graphene tribotronics for electronic skin and touch screen applications. *Adv Mater*. 2017;29:1603544.
91. Cho KG, An S, Cho DH, et al. Block copolymer-based supramolecular ionogels for accurate on-skin motion monitoring. *Adv Funct Mater*. 2021;31:2102386.
92. Fu X, Zhuang Z, Zhao Y, et al. Stretchable and self-powered temperature–pressure dual sensing ionic skins based on thermogalvanic hydrogels. *ACS Appl Mater Interfaces*. 2022;14:44792-44798.
93. Lu Y, Qu X, Wang S, et al. Ultradurable, freeze-resistant, and healable MXene-based ionic gels for multi-functional electronic skin. *Nano Res*. 2022;15:4421-4430.
94. You I, Mackanic DG, Matsuhisa N, et al. Artificial multimodal receptors based on ion relaxation dynamics. *Science*. 2020;370:961-965.
95. Pu J, Zhang Y, Wada Y, et al. Fabrication of stretchable MoS_2 thin-film transistors using elastic ion-gel gate dielectrics. *Appl Phys Lett*. 2013;103:023505.
96. Oh G, Kim J-S, Jeon JH, et al. Graphene/pentacene barristor with ion-gel gate dielectric: flexible ambipolar transistor with high mobility and on/off ratio. *ACS Nano*. 2015;9:7515-7522.
97. Ren Y, Yuan H, Wu X, et al. Direct imaging of nanoscale conductance evolution in ion-gel-gated oxide transistors. *Nano Lett*. 2015;15:4730-4736.
98. Hu H, Zhai F, Hu D, et al. Broadly tunable graphene plasmons using an ion-gel top gate with low control voltage. *Nanoscale*. 2015;7:19493-19500.
99. Choi Y, Kang J, Secor EB, et al. Capacitively coupled hybrid ion gel and carbon nanotube thin-film transistors for low voltage flexible logic circuits. *Adv Funct Mater*. 2018;28:1802610.
100. Kong L, Sun J, Qian C, Wang C, Yang J, Gao Y. Spatially-correlated neuron transistors with ion-gel gating for brain-inspired applications. *Org Electron*. 2017;44:25-31.
101. Lee J, Aida T. "Bucky gels" for tailoring electroactive materials and devices: the composites of carbon materials with ionic liquids. *Chem Commun*. 2011;47:6757-6762.
102. Liu Z, Li B, Liu YD, Liang Y. Integrated bending actuation and the self-sensing capability of poly(vinyl chloride) gels with ionic liquids. *Adv Funct Mater*. 2022;32:2204259.
103. Vinh Quy VH, Kim K-W, Yeo J, et al. Tunable electrochromic behavior of biphenyl poly (viologen)-based ion gels in all-in-one devices. *Org Electron*. 2022;100:106395.
104. Oh H, Seo DG, Yun TY, Lee SB, Moon HC. Novel viologen derivatives for electrochromic ion gels showing a green-colored state with improved stability. *Org Electron*. 2017;51:490-495.
105. Moon HC, Lodge TP, Frisbie CD. Electrochemiluminescent displays based on ion gels: correlation between device performance and choice of electrolyte. *J Mater Chem C*. 2016;4:8448-8453.
106. Kushida S, Kebrich S, Smarsly E, Strunk K-P, Melzer C, Bunz UHF. Light-emitting electrochemical cells based on

conjugated ion gels. *ACS Appl Mater Interfaces*. 2020;12:38483-38489.

107. Kim JW, Myoung JM. Flexible and transparent electrochromic displays with simultaneously implementable subpixelated ion gel-based viologens by multiple patterning. *Adv Funct Mater*. 2019;29:1808911.

AUTHOR BIOGRAPHIES

Dr. Naiwei Gao received his BS degree from the School of Advanced Materials and Nanotechnology, XiDian University, in 2015. He then received his PhD degree from the Department of Chemistry, Renmin University of China, in 2020. Currently, he is pursuing postdoctoral research work at the College of Physics and Optoelectronic Engineering, Shenzhen University. His research focuses on the functional derivation of ionic materials and their applications in high-performance flexible electronic devices.

Dr. Caofeng Pan received his BS degree (2005) and his PhD (2010) in Materials Science and Engineering from Tsinghua University, China. He then joined the Georgia Institute of Technology as a postdoctoral fellow. He is a professor and group leader at the Beijing Institute of Nanoenergy and Nanosystems, Chinese Academy of Sciences, since 2013. His main research interests focus on the fields of low-dimensional materials for fabricating smart electronic and optoelectronic devices for tactile sensing.

How to cite this article: Gao N, Pan C. Intelligent ion gels: design, performance, and applications. *SmartMat*. 2023;e1215. doi:10.1002/smm2.1215